Chapter One

Introduction

1.1 General Review

About 3.2 billion people are at high risk of malaria globally, 350 million have the parasite in their body and 198 million were ill with malaria in 2013 with almost 584 000 dying as a result - WHO. (Some new research suggests that 1.24 million died of malaria in 2010 with 85% of the deaths in Sub Saharan Africa) (The official figures for 2010 were much lower: 216 million ill and 655 000 who died from malaria). This is the most important parasitic disease in the world. Between 2000 and 2012 3.3 million deaths have been averted by new efforts. [1]

The majority of countries in tropical Sub-Saharan Africa (SSA) have a reduction of their potential income by between 1-1.3% per year due malaria and that over a 15 year period this loss of income amounts to almost 20% of their potential earnings. Put in another way probably 20% of their poverty is due to malaria. In the worst affected countries malaria accounts for 40% of public health expenditure, 30-50% of in-patient admissions and up to 60% of out-patient clinic visits. In 1997 it was estimated at the Global Malaria Conference in Hydrabad that annual deaths from malaria were between 2.5 million and 3.5 million. [1]

Initiation of malaria treatment largely depends on good, laboratory confirmed diagnosis. This project focuses on quantify the type of malaria parasite (hemozoin) presented in blood stream by measuring the property of light interaction with hemozoin crystal absorption of laser beam when interacting with hemozoin particles on application of a magnetic field in a non-invasive way.

Parasite Types

There are 4 main types of parasites: Plasmodium falciparum, P. malariae, P. ovale, and P. vivax. (P. knowlesi is found on Borneo and parts of peninsular Malaysia) Plasmodium falciparum is virtually the only life-threatening type and is also the dominant type in most parts of tropical Africa. In Zambia this type accounts for 95% of all malaria. In many parts of Asia the malaria threat is smaller than in Africa and P. vivax is dominant in many countries (India, Pakistan, and Sri Lanka etc.) Only P. vivax and P. ovale can have a long-term liver stage where the parasite can hide for several years and flare-up again. This stage needs special treatment with primaquine to clear the parasite. [1]

Hemozoin

When the Malaria parasite ingests the hemoglobin of the red blood cell, it sequesters the toxic iron inside of its abdominal vacuole for safety. The iron atoms reside in a carbon containment structure and link together to make up the hemozoin crystals. [20]

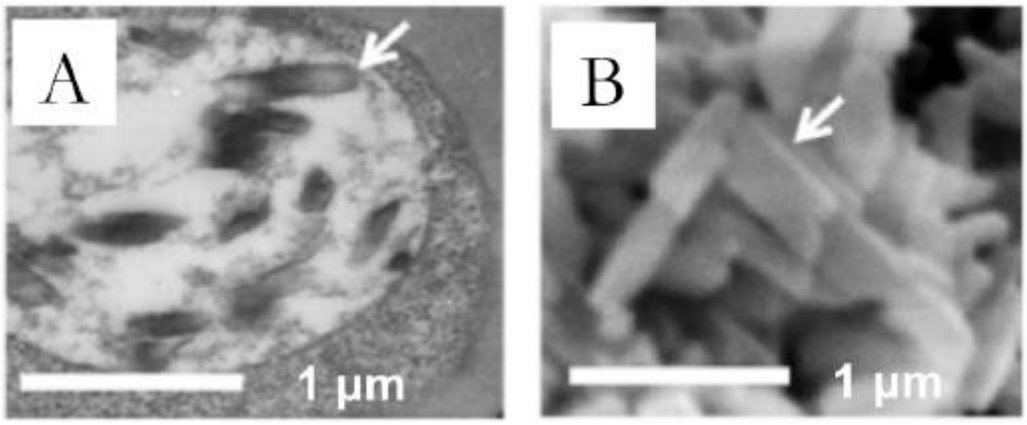

Figure (1-1): a) Structure off Hemozoin, b) Micrographs of hemozoin (indicated by white arrows). [20]

Hemozoin Production

Inside the body, the malaria parasites target the red blood cells as their hosts. Once inside, the parasite digests the hemoglobin and breaks it down into proteins and hemes, protein structures with iron cores that are used by the blood to carry oxygen throughout the body. The parasite then sequesters the iron cores into carbon containers and connects them together with hydrogen bonds. The containers tend to line up such that they form a needle structure within the parasite. Once the parasite moves on to a new blood cell, it leaves the previous cell's needles, now called hemozoin, in the bloodstream, where they can be detected. [20]

1.2 Problem Statement

Malaria is confirmed to be a serious disease by laboratories. Some methods which use in malaria detection are limited in detecting type of malaria, varying at accuracy depending mainly on the skill base of laboratory technicians, time consuming and not applicable at all environments.

1.3 Objectives

The general objective is to apply magneto-optical technique (MOT) to identify malaria parasite.

The specific objectives are to

1. test all plasmodium species; for distinguishing type of malaria, with more volunteers than previous researches.
2. achieve high accuracy, less pain and high performance with small duration of time.

1.4 Methodology

The methodology focuses on design and implementation of portable prototype to detect all types of malaria parasite depending on basis of Magneto-Optical Technique (MOT) [using a magnetic field and laser "Infrared waves"] and embedded systems, by detecting IR LASER beam passing through human finger or blood sample using a data acquisition system to acquire the signal from human finger.

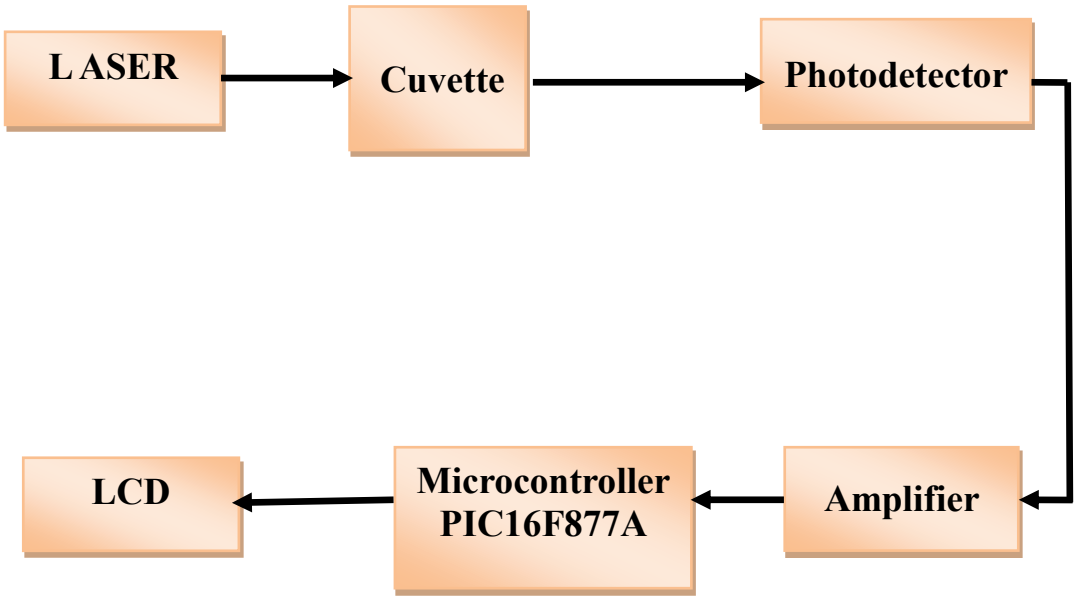

Figure (1-2): Methodology block diagram

1.5 Thesis Layout

This thesis consists six chapters, chapter one is introduction. Literature reviews is introduced in chapter two. Chapter three illustrates theoretical background. The proposed system is discussed in chapter four. Chapter five describes results and discussion. Finally Chapter six contains conclusion and future recommendations.

Chapter Two

Literature Review

Several approaches to the diagnosis of malaria can be adopted. Each approach presents characteristics such as cost, ease of performance and accuracy, which will determine its applicability to different situations.

2.1 Microscopic Diagnosis

Payne D. Use and limitations of light microscopy for diagnosing malaria at the primary health care level, 1988.

Conventional light microscopy is the established method for the laboratory confirmation of malaria. The careful examination by an expert microscopist of a well prepared and well stained blood film remains currently the "gold standard" for detecting and identifying malaria parasites. In most settings, the procedure consists of: collecting a finger-prick blood sample; preparing a thick blood smear (in some settings a thin smear is also prepared); staining the smear (most frequently with Giemsa); and examining the smear through a microscope (preferably with a 100X oil immersion objective) for the presence of malaria parasites. [4]

2.2 Rapid Diagnostic Tests (RDTs)

Joel C. Mouatcho and J. P. Dean Goldring , Malaria rapid diagnostic tests: challenges and prospects , 2013.

This study shows that RDTs use immunochromatography, whereby a colored detecting antibody binds to lysed parasite antigen and is carried by capillary action on a nitrocellulose strip and arrested by a capture antibody, resulting in a colored band on a test strip. RDTs are simple and easy to use with little expertise required for interpretation, although some training improves interpretation. RDTs are generally available in easily

transportable strips and do not require a source of electricity; thus, they are suitable for field tests and for use by travelers or tourists. A result is obtained within a few minutes. Although not suitable, at present, for qualitative outcomes, RDTs are very useful in endemic areas where many people can be screened in a short period of time. [5]

2.3 ELISA (The Enzyme-Linked Immunosorbent Assay)

Robert H. Yolken, Enzyme Immunoassays for the Detection of Infectious Antigens in Body Fluids: Current Limitations and Future Prospects, 1982.

This work showed that enzyme immunoassays are attaining increased usage for the direct detection of microbial antigens in body fluids. Advantages of enzyme immunoassays include a high degree of sensitivity resulting from the inherent magnification of the enzyme-substrate reaction and the use of objective end points without the need for radioactivity. Enzyme immunoassays have been developed for the reliable detection of several important microbial antigens in body fluids, including antigens of rotavirus, hepatitis B virus, and Haemophilus influenzae type b. However, standard enzyme immunoassay techniques are not sufficiently sensitive for the measurement of some antigens from other viruses, bacteria, and parasites in concentrations that commonly occur in body fluids during the course of infectious diseases. [6]

The ELISA lack is due to that species-specific antibodies are detectable in the blood some days after parasite invasion of the bloodstream and may persist for long periods of time after infection has occurred. The ELISA test format is representing in the following figure.

Figure (2-1): ELISA Test [7]

2.4 PCR (Polymerase Chain Reaction)

Peipei Li, Zhenjun Zhao, Ying Wang and et al, Nested PCR detection of malaria directly using blood filter paper samples from epidemiological surveys, 2011

In this study a simplified PCR method was developed to directly use a small blood filter paper square (2 × 2 mm) as the DNA template after treatment with saponin. This filter paper-based nested PCR method (FP-PCR) was compared to microscopy and standard nested PCR with DNA extracted by using a Qiagen DNA mini kit from filter paper blood spots of 204 febrile cases. The FP-PCR technique was further applied to evaluate malaria infections in 1,708 participants from cross-sectional epidemiological surveys conducted in Myanmar and Thailand. The FP-PCR method had a detection limit of ~0.2 parasites/μL blood, estimated using cultured Plasmodium falciparum parasites. With 204 field samples, the sensitivity of the FP-PCR method was comparable to that of the standard nested PCR method, which was significantly higher than that of microscopy. Application of the FP-PCR method in large cross-sectional studies conducted in Myanmar and Thailand detected 1.9% (12/638) and 6.2% (66/1,070) asymptomatic Plasmodium infections, respectively, as

compared to the detection rates of 1.3% (8/638) and 0.04% (4/1,070) by microscopy. This FP-PCR method was much more sensitive than microscopy in detecting Plasmodium infections. It drastically increased the detection sensitivity of asymptomatic infections in cross-sectional surveys conducted in Thailand and Myanmar, suggesting that this FP-PCR method has a potential for future applications in malaria epidemiology studies. [8]

2.5 Automatic Malaria Diagnosis Based on Giemsa Stained Blood Smear Images

Computer Vision for Microscopy Diagnosis of Malaria

F.Boray Tek, Andrew.G Dempster , and Izzet Kale, Computer vision for microscopy diagnosis of malaria, 2009.

This paper reviews computer vision and image analysis studies aiming at automated diagnosis or screening of malaria infection in microscope images of thin blood film smears. Existing works interpret the diagnosis problem differently or propose partial solutions to the problem. A critique of these works is furnished. In addition, a general pattern recognition framework to perform diagnosis, which includes image acquisition, pre-processing, segmentation, and pattern classification components, is described. The open problems are addressed and a perspective of the future work for realization of automated microscopy diagnosis of malaria is provided. [21]

Recognition of Blood Cell Images Based on Color Fuzzy Clustering

En yong wang, Zhen gpin gou, Ai-min miao and et al, Recognition of Blood Cell Images Based on Color Fuzzy Clustering, 2009.

In this paper, a method based on the color fuzzy clustering was proposed to divide the color areas and distribute each pixel into each area. Since red

cells, leukocytes, platelets, and cytoplasm had different color in the blood cell image, they were extracted according to their own colors. First, the color areas of red cells, leukocytes, platelets and cytoplasm were determined, respectively. Second, pixels were distributed into each color area by using the fuzzy clustering algorithm. The proposed method was implemented by Java program. Five blood cell images were used in the test. The leukocytes, platelets, and red cells were detected accurately in all five images. Results demonstrated the effectiveness of the proposed method. [17]

Malaria Diagnose Using Neural Network Architecture

Ahmed elmubarak Bashir, Zeinab A.Mustafa, Islah Abdelhameid, Rimaz Ibrahem , Detection of Malaria Parasites Using Digital Image Processing 2017.

In this work, an accurate, rapid and affordable model of malaria diagnosis using stained thin blood smear images was developed. The method made use of the intensity features of Plasmodium parasites and erythrocytes. Images of infected and non-infected erythrocytes were acquired, pre-processed, relevant features extracted from them and eventually diagnosis was made based on the features extracted from the images. A set of features based on intensity have been proposed, and the performance of these features on the red blood cell samples from the created database have been evaluated using an artificial neural network (ANN) classifier. The results have shown that these features could be successfully used for malaria detection.[18]

2.6 Non-invasive Malaria Diagnose Methods

Detection of malaria using human saliva

Wilson NO, Adjei AA, Anderson W and et al, Detection of Plasmodium falciparum histidine-rich protein II in saliva of malaria patients, 2004.

According to this paper, detection of *Plasmodium falciparum* parasites in patients with malaria necessitates drawing blood, which increases the risk of accidental infections and is poorly accepted in communities with blood taboos. Thus, non-invasive, cost-effective malaria tests that minimize the need for blood collection are needed. *Plasmodium falciparum* histidine-rich protein II (*PfHRP* II) levels in plasma and saliva were compared in malaria–positive and –negative patients in Ghana. Plasma and saliva obtained from 30 thick-film positive and 10 negative children were evaluated for *PfHRP* II by ELISA. Among the 30 children with positive blood smear, 16 (53%) were *PfHRP* II positive in plasma and 13 (43%) had *P*fHRP II positive saliva. The sensitivity of *PfHRP* II detection was 53% for plasma and 43% for saliva. The specificity was 100% with no false positive for both plasma and saliva when compared with blood smear. Thus, rapid detection of *PfHRP* II antigen in saliva may be a useful non-invasive and cost-effective malaria diagnostic technique.[10]

The Detection of Plasmodium Falciparum in Human Saliva Samples using PCR

Ofentse Jacob Pooe, The detection of Plasmodium falciparum in human saliva samples, 2011.

This study was sought to establish the constituents of human saliva that harbours parasite DNA in malaria infected subjects. Furthermore the study optimized the use of Saliva as an alternative malaria DNA source in malaria infected patients. A total of 88 subjects were enrolled in this study,

35 (40, 7 %) were males and 51 (59, 3 %) were females. The age range was from 3 months to 99 years old (mean = 29.6 years; median = 18 years). Blood was drawn from each subject for subsequent use in microscopic examination and PCR tests. Saliva samples were also collected for PCR on Saliva derived parasite DNA. DNA was extracted using commercial kit on different saliva fractions from 46 malaria positive (thick film positive & blood PCR positives) individuals and 45 malaria negative individuals. Nested PCR was used to amplify malaria the *Plasmodium falciparum* dihydrofolate reductase (*pfdhfr*) gene. Generally PCR conducted on DNA purified from both blood and saliva was more sensitive than conventional microscopy, as previously reported. The pellet fraction of saliva was a more reliable and sensitive source of amplifiable parasite DNA compared to the soluble saliva fraction. After PCR optimization amplification was enhanced 94.1% (sensitivity) and 97% (specificity) against DNA derived from blood as the gold standard. This study further confirms that saliva samples are a reliable non-invasive alternative to blood for the PCR detection of malaria, as previously reported. The source of DNA was primarily in the pellet fraction though; however, refinement is still needed to identify the exact source of DNA in that fraction. [9]

PCR Detection of Plasmodium Falciparum in Human Urine Samples

Kwannan Nantavisai, Malaria detection using non-blood samples, 2014.

As mentioned in this paper urine is another sample which has been assessed for non-invasive malaria detection. Previous studies suggested that both malarial antigens and antibodies are possibly released into the urine during malaria infection. An ultrastructural pathological study of renal tissue from *P. falciparum* patients revealed the presence of parasitized erythrocytes sequestered in glomerular and tubulointerstitial

vessels and also immune complexes including IgG, C3, and malarial antigens. These results along with proteinuria reported in patients infected with *P. falciparum* lead to the idea that parasite antigens and antibodies may be excreted into urine. Antisera raised against urine from *P. falciparum* patients showed positive results with *P. falciparum* parasites in indirect immunofluorescence test and immunoprecipitated extracts of parasites metabolic. These results suggest that a variety of malarial antigens are released into urine. Moreover, dot-blot and western blot assay also revealed the presence of malarial antigens in urine of patients infected with *P. vivax*. It should be noted however that the antigens can still be detected in patients who no longer had detectable parasitemia after treatment. [11]

Transdermal Diagnosis of Malaria Using Vapor Nanobubbles Lukianova-Hleb, E., Bezek , T. Hurrell, A.Lapotko and et al , Transdermal Diagnosis of Malaria Using Vapor Nanobubble , 2015.

In this paper A fast, precise, noninvasive, high-throughput, and simple approach for detecting malaria in humans and mosquitoes is not possible with current techniques that depend on blood sampling, reagents, facilities, tedious procedures, and trained personnel. We designed a device for rapid (20-second) noninvasive diagnosis of *Plasmodium falciparum* infection in a malaria patient without drawing blood or using any reagent. This method uses transdermal optical excitation and acoustic detection of vapor nanobubbles around intraparasite hemozoin.

The same device also identified individual malaria parasite infected Anopheles mosquitoes in a few seconds and can be realized as a low-cost universal tool for clinical and field diagnoses. [19]

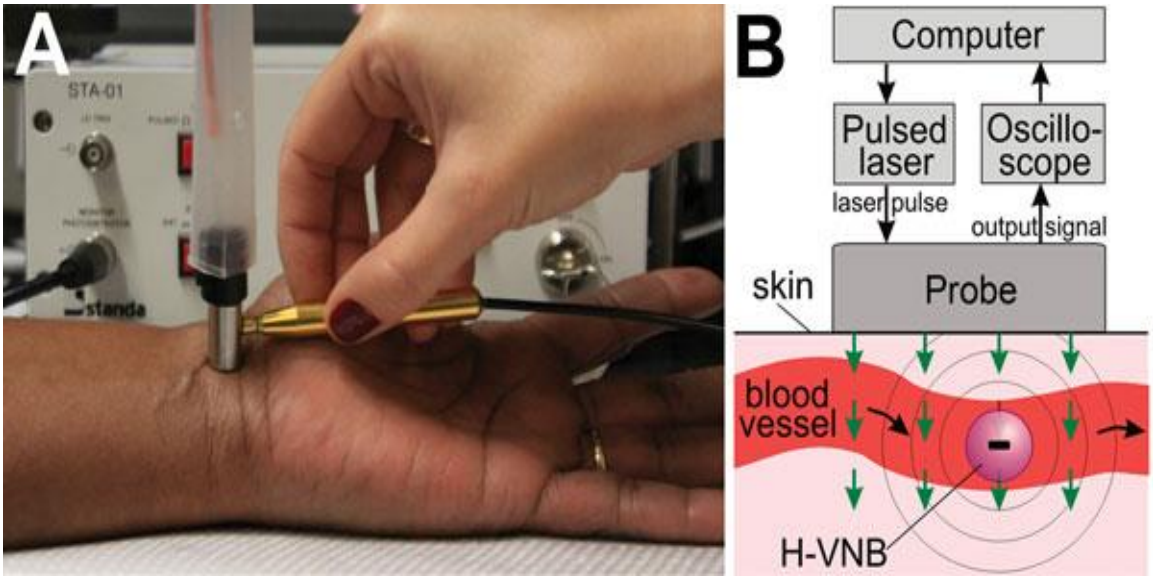

Figure (2-2): Experimental laboratory prototype of a malaria diagnostic device with the pulsed laser and the integrated probe shown being scanned across a human wrist. [19]

Chapter Three

Theoretical Background

This chapter reviews briefly the absorption and scattering characteristics of biological subjected to infrared using magneto optical technology. Also gives clarification of some terms and concepts which will be used in next chapters. During this project units of nm will be used to express the wavelength in addition to a general perspective of IR spectroscopy. The principle of Magneto Optical Technology (MOT), which are the basis of this thesis, are also discussed.

3.1 Background

Malaria has been around since ancient times. The early Egyptians wrote about it on papyrus, and the famous Greek physician Hippocrates described it in detail. [2]

The name is derived from the Italian, “mal aria,” or bad air. In (1880), the French scientist Alphonse Laveran discovered the real cause of malaria, the single-celled Plasmodium parasite. Almost (20) years later, scientists working in India and Italy discovered that Anopheles mosquitoes are responsible for transmitting malaria .In World War II and the Vietnam War, more personnel time was lost due to malaria than to bullets.

3.2 Malaria Parasite Life Cycle

Malaria is spread by the bite of the female Anopheles mosquito (45 species are important vectors with A. gambiae being the most effective) in which the parasite goes through a complicated lifecycle ending up in the salivary glands. A bite from a mosquito infected with such parasites is accompanied by the injection of saliva to stop the blood from clotting.

With the saliva are injected parasites at the sporozoite stage where they can spread within 45 minutes through the blood stream of man and reach the hepatocytes of the liver. They bore into these hepatocytes and start asexual reproduction into schizonts and finally discharge merozoites into the blood stream. In Plasmodium falciparum (the main malaria parasite in Tropical Africa) the liver stage lasts 5.5 days. In P. malariae it lasts 15 days. [1]

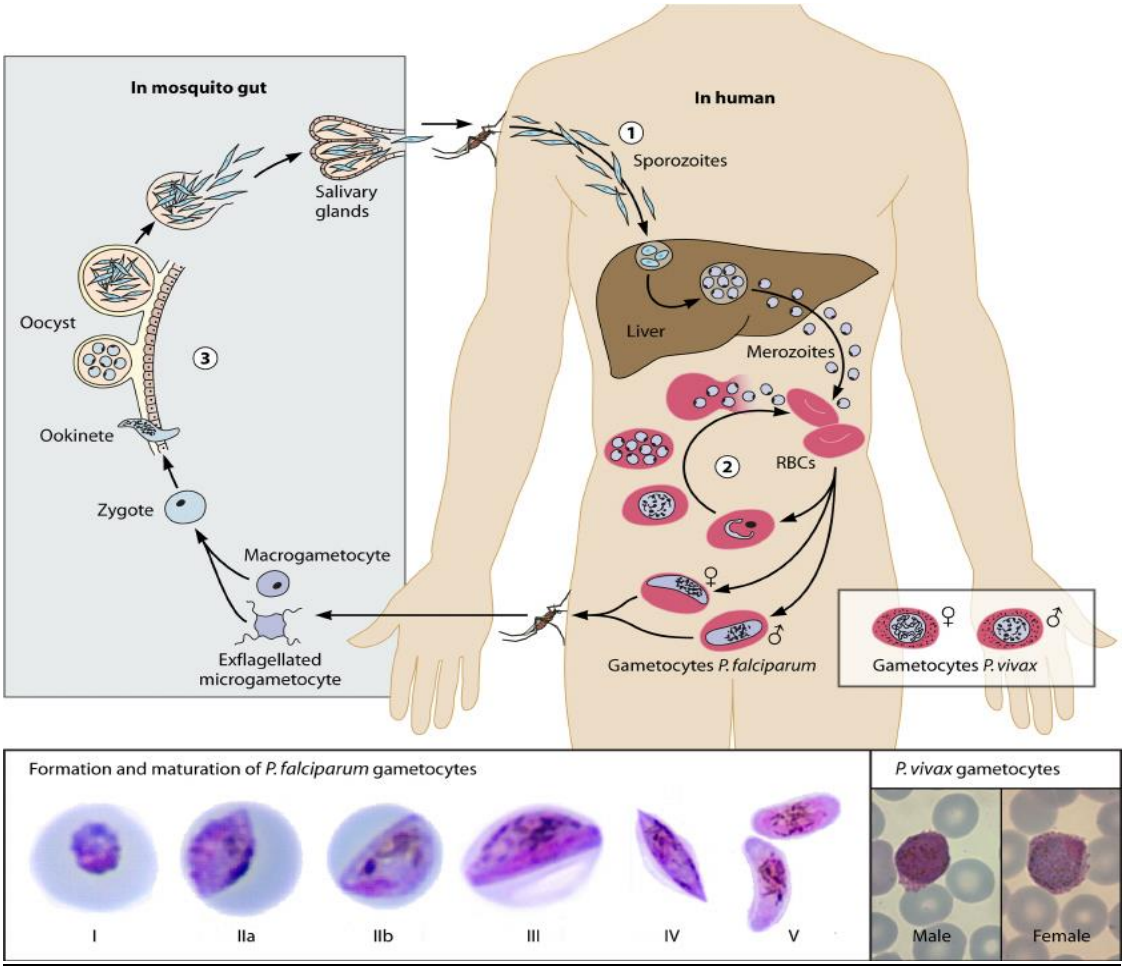

Figure (3-1): Malaria parasite life cycle. [22]

The merozoites bore into red cells and form a vacuole with the invaginated red cell membrane. About 36 hours (54 hrs. in P.malariae) after invasion repeated nuclear division forms a schizont or better termed a meront and finally the growing parasite fills the red cell and is packed with merozoites. It then bursts and 6-36 merozoites are released to invade red

blood cells. The infection expands logarithmically at around 10-fold per cycle. The release of several substances at this bursting stage brings about the symptoms of malaria which include fever, headache, and pain in muscles, nausea and vomiting. Finally, if untreated, so many red blood cells are damaged that the person becomes anemic due to lack of intact blood cells. The spleen which is the dumping ground of broken down red cells may become enlarged and tender. The person may even become jaundiced as the break down products of hemoglobin finally overwhelm the liver's capacity to deal with them, and the inflammatory effect of malaria on the liver cells function. After a series of asexual cycles in P.falciparum a sub-population of the parasite develops into sexual forms (gametocytes) with the process taking about 7-10 days. This is the stage that is then taken up by the female anopheles. The parasite then goes through the complex process within the mosquito which brings us back to our starting point as sporozoites in the salivary glands. [1]

Malaria is caused by five species of the parasite belonging to the genus Plasmodium. Four of these – P. falciparum, P. vivax, P. malariae and P. ovale – are human malaria species, which are spread from one person to another by female mosquitoes of the genus Anopheles. [4]

Plasmodium falciparum is responsible for most malaria deaths, especially in Africa. The infection can develop suddenly and produce several life threatening complications. With prompt, effective treatment, however, it is almost always curable [2].

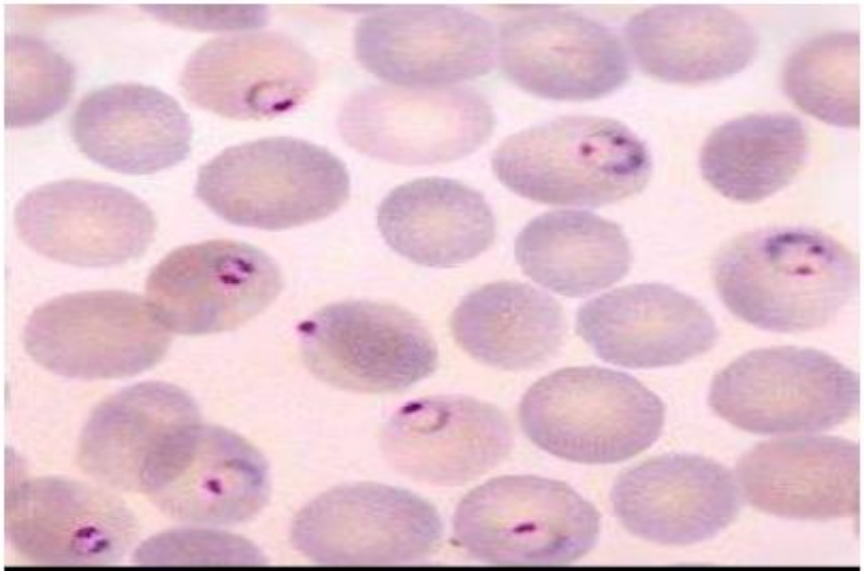

Figure (3-2): Parasited red blood cells “Falciparum trophozoites” [23]

Plasmodium vivax the most geographically widespread of the species, produces less severe symptoms. Relapses**,** however, can occur for up to (3) years, and chronic disease is debilitating. Once common in temperate climates, P. vivax is now found mostly in the tropics, especially throughout Asia [2].

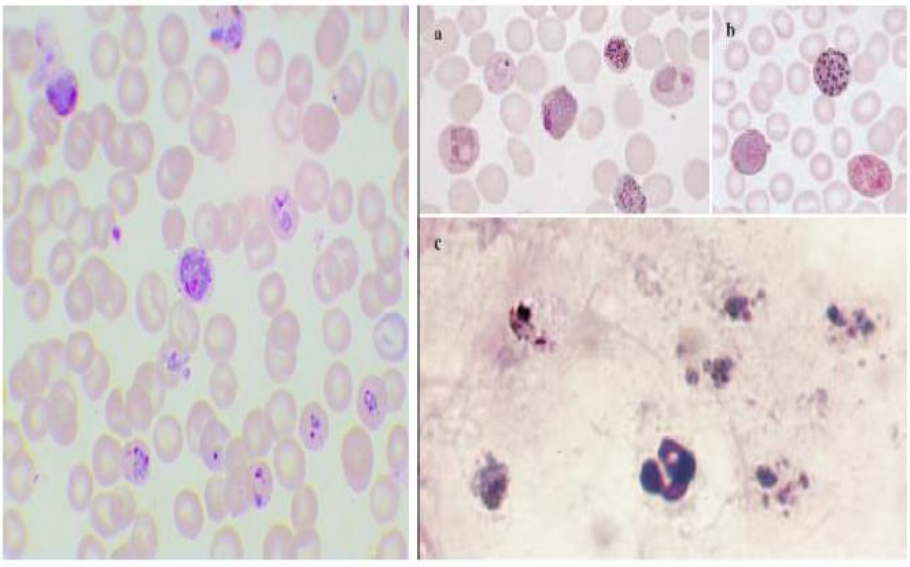

Figure (3-3): P. vivax gametocytes/schizont,
Gametocytes: spherical shaped. [24]

Plasmodium malariae infections not only produce typical malaria symptoms but also can persist in the blood for very long periods, possibly decades, without ever producing symptoms. A person with asymptomatic (no symptoms) P. malariae, however, can infect others, either through blood donation or mosquito bites. P. malariae has been wiped out from temperate climates, but it persists in Africa [2].

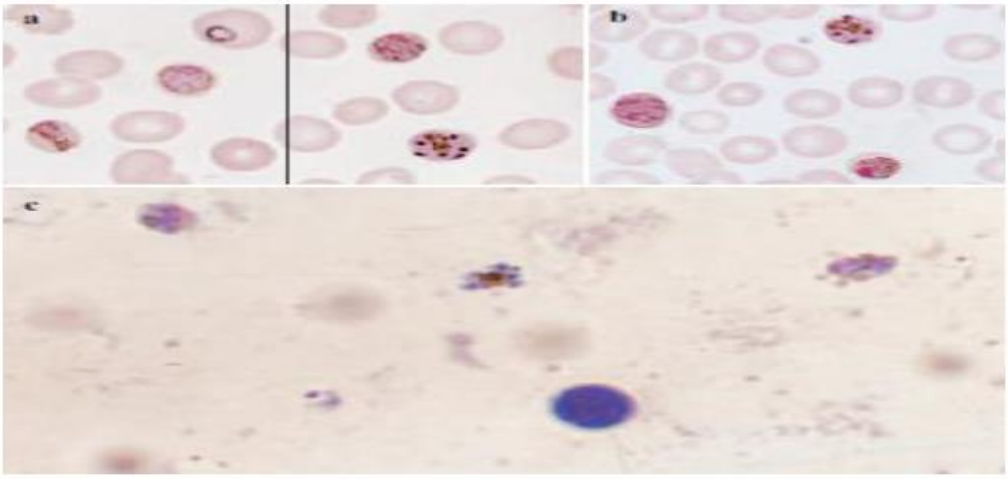

Figure (3-4): P. malariae, Band shaped trophz. [25]

Plasmodium ovale is rare, can cause relapses, and generally occurs in West Africa [2].

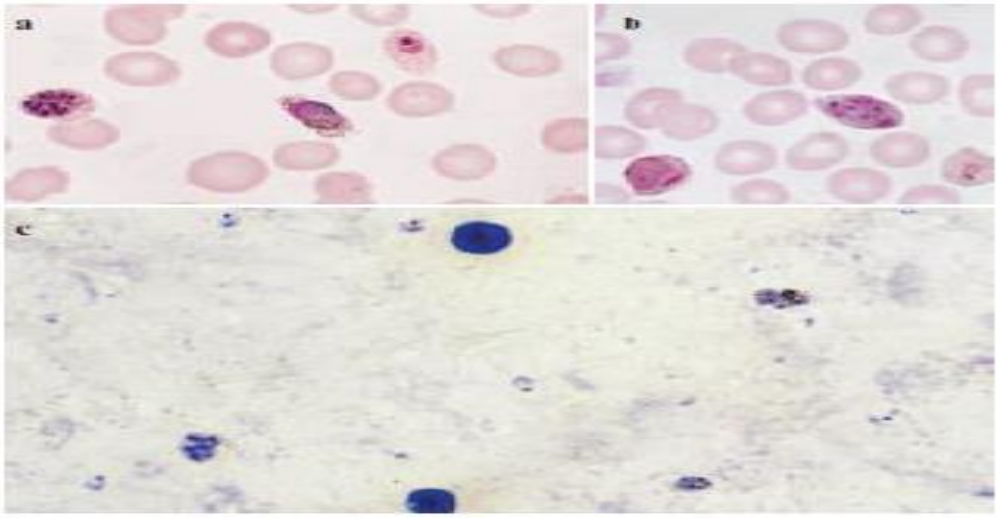

Figure (3-5): P.ovale, a) Trophz compact and rounded not amoeboid , b) schizonts and gametocyte similar to P.vivax , c)Number of merozoite 6-12 RBC young.[25]

3.3 Clinical Signs and Symptoms of Malaria

The disease is reasonably easy to recognize in people who have not had malaria before, or have had few attacks. The common symptoms of malaria are: high fever, headache, severe chills or rigor, profuse sweating and general body pains. Some patients may have vomiting, cough or diarrhea. In persistent and recurrent infections, anemia may be present. [3] As similar clinical signs are seen in other common diseases, further investigations are necessary before a reliable diagnosis of malaria can be made. The clinical presentation of malaria is even less clear in patients who have had a number of malaria attacks, as they generally show no clear signs or symptoms. Care must also be taken to establish whether the patient has taken antimalarial medicines before going to hospital, as this can modify the clinical presentation. Previous treatment with antimalarial medicines, by reducing the parasite density to very low levels, may make microscopic diagnosis more difficult. Knowing which treatment was received is important in order to avoid an overdose of antimalarial medicines, which can be dangerous, especially if the patient was unconscious when admitted to hospital. [3]

3.4 Disease Situations

There are four situations of malaria threat that are so different from each other that it is as if four different diseases are being described:

High transmission with an extremely effective vector (Anopheles gambiae) of P. falciparum. Here malaria will almost certainly be the main cause of morbidity and mortality in children under 5 and the main cause of illness amongst adults. Chloroquine treatment is virtually always useless. Impregnated mosquito nets and more effective treatment are the only hope in the community.

Low transmission of P. falciparum. Here the disease may occasionally come as epidemics (e.g. during El Nino-associated climate changes) that are a threat to the life and health of both adults and children with massive outbreaks of severe anemia and cerebral malaria during the outbreaks but little impact otherwise. In an outbreak, there may even be discussion about short-term prophylaxis for children and pregnant women, as well as impregnated mosquito nets and early effective treatment.

Moderate transmission of P. vivax and ovale. Here both prophylaxis and treatment with chloroquine are usually effective but follow-up treatment of the liver stage with primaquine is still needed. Environmental changes such as draining marshlands and separating human from animal dwellings often make a big impact.

Low transmission of P. vivax, ovale and malariae. Here malaria is an exotic disease without much impact at the community level. [1]

3.5 Optical Properties of Biological Tissues

The optical properties of a tissue are described in terms of absorption, scattering, reflection and refraction as shown in figure (3-6).

Optical absorption: Is a process where the energy of a light photon is taken up by a molecule without the re-emission of another photon.

Optical scattering is an interaction of light as it passes through matter, in which the direction of the incident rays is changed by molecules or small particles present in the medium. Scattering plays an important role in the spatial distribution of absorbed energy. At the longer wavelengths (red and near infra-red) where the light is absorbed less, the beam is more penetrating (ignoring scattering effects).

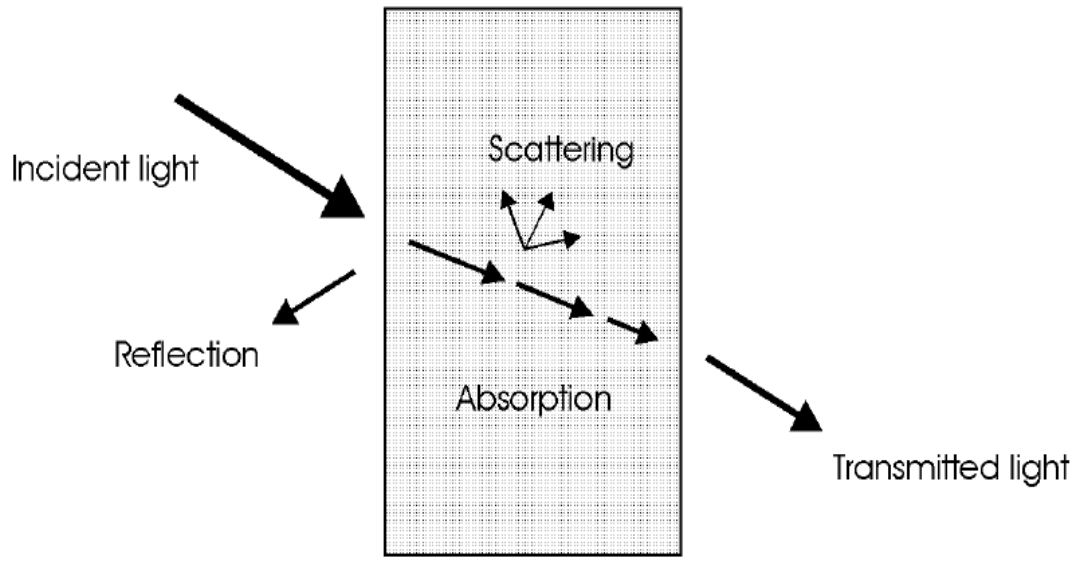

Figure (3-6): Geometry of reflection, refraction, absorption, and scattering.[12]

3.5.1 Absorption Theory

Two laws are frequently applied which describe the effect of either thickness or concentration on absorption, respectively. They are commonly called Lambert's law and Beer's law, and are expressed by

$$I_z = I_0 \exp(-\alpha z) , \qquad (3\text{-}1)$$

And

$$I_z = I_0 \exp(-k' c z) , \qquad (3\text{-}2)$$

Where z denotes the optical axis, I_z is the intensity at a distance z, I_0 is the incident intensity, α is the absorption coefficient of the medium, c is the concentration of absorbing agents, and k' depends on internal parameters other than concentration. Since both laws describe the same behavior of absorption, they are also known as the Lambert–Beer law. From (3-1), we obtain

$$z = \frac{1}{\alpha} \ln \frac{I_0}{I_z} . \qquad (3\text{-}3)$$

The inverse of the absorption coefficient α is also referred to as the absorption length L, i.e.

$$L = \frac{1}{\alpha}. \qquad (3\text{-}4)$$

The absorption length measures the distance z in which the intensity I_z has dropped to 1/e of its incident value I_0. [12]

The ratio of the intensity at a distance (I_z) to the incident intensity (I_0) is called the transmittance T:

$$T = I_z / I_0 \qquad (3\text{-}5)$$

Absorbance (A), then, is defined as the logarithm (base 10) of the reciprocal of the transmittance:

$$A = -\log T = \log (1/T) \qquad (3\text{-}6)$$

In a spectrophotometer, monochromatic plane-parallel light enters a sample at right angles to the plane-surface of the sample. In these conditions, the transmittance and absorbance of a sample depends on the molar concentration (c), light path length in centimeters (L), and molar absorptivity (ε) for the dissolved substance. [13]

$$T = 10^{\varepsilon cL} \text{ or } A_\lambda = \varepsilon cL \qquad (3\text{-}7)$$

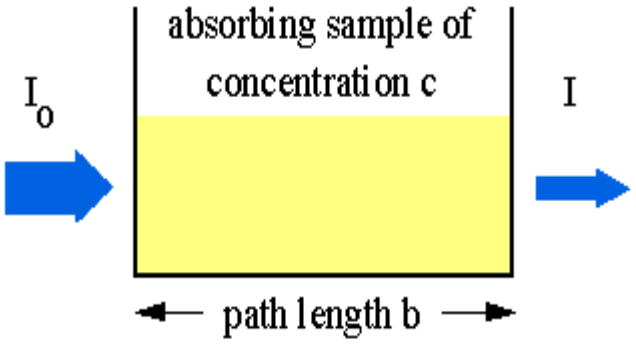

Figure (3-7): Light travels through the medium as absorption interaction.

Beer's Law states that molar absorptivity is constant and the absorbance is proportional to concentration for a given substance dissolved in a given solute and measured at a given wavelength. [14]

Accordingly, molar absorptivities are commonly called molar extinction coefficients. Since transmittance and absorbance are unit less, the units for molar absorptivity must cancel with units of measure in concentration and light path. Accordingly, molar absorptivities have units of $M^{-1}cm^{-1}$. Standard laboratory spectrophotometers are fitted for use with 1 cm width sample cuvettes; hence, the path length is generally assumed to be equal to one and the term is dropped altogether in most calculations.

$$A_\lambda = \varepsilon\, c\, L = \varepsilon\, c \qquad \text{when } L = 1 \text{ cm} \qquad (3\text{-}8)$$

Absorption Characteristics of Blood

The major contribution to blood optical absorption is due to hemoglobin, both in its oxygenated and deoxygenated forms. The absorption spectrum for deoxy-hemoglobin and oxy-hemoglobin are distinctly different, thus resulting in difference in total absorption as a function of oxygen saturation. The absorption spectrum of oxy-hemoglobin peaks between 400 nm and 600 nm and deoxy-hemoglobin peaks between 400 nm and 850 nm. The absorption coefficient of whole blood is represented in figure (3-8) which shows fully oxygenated and deoxygenated blood. Reliable data beyond 1000 nm wavelength is difficult to find in the literature. Beyond 1000 nm water absorption figure (3-8) might begin to dominate over hemoglobin absorption. [15]

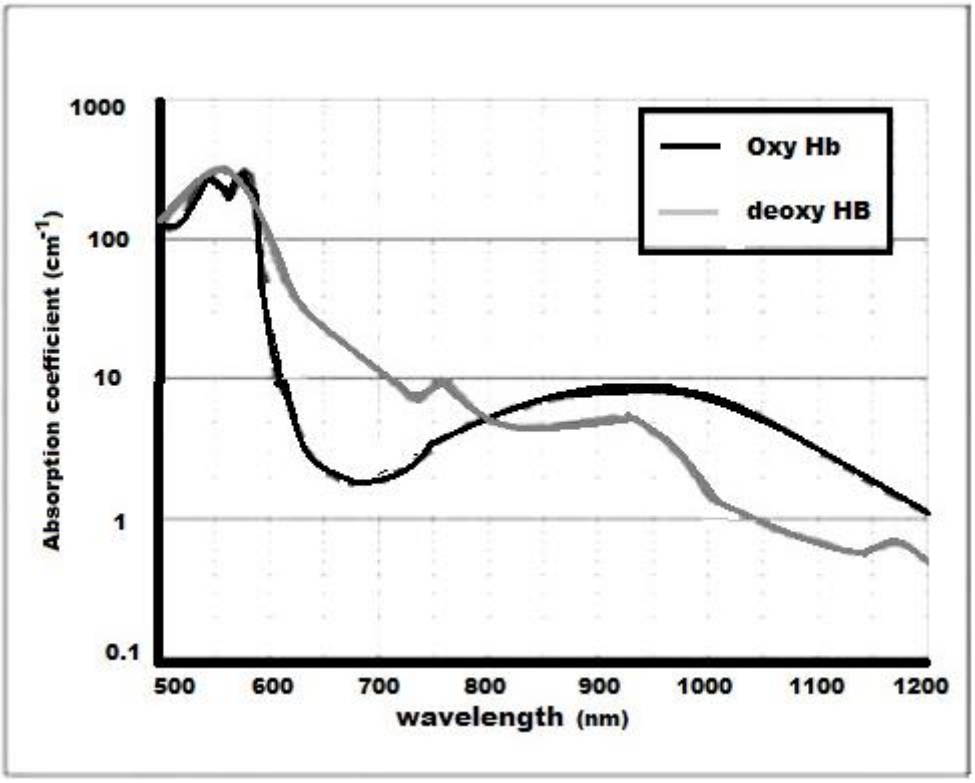

Figure (3-8): Hemoglobin absorption coefficient in the range 500-1200 nm. [15]

Absorption spectra of oxygenated (HbO2) and de-oxygenated (Hb) forms of hemoglobin are somewhat different – hence the difference in color between arterial and venous blood. [16]

Absorption Characteristics of Water

The skin is composed of approximately 70% water and the volume of water presents a large absorption target even for wavelengths of light that have a fairly low water absorption coefficient.[16]

Although water is nearly transparent in the range of visible light, it becomes absorbing over the near-infrared region. Water is a critical component since its concentration is high in human tissue. The absorption spectrum of water in the range 500-1200 nm is shown in figure (3-9). Although absorption is rather low in this spectral range, it still contributes to the overall tissue attenuation. [15]

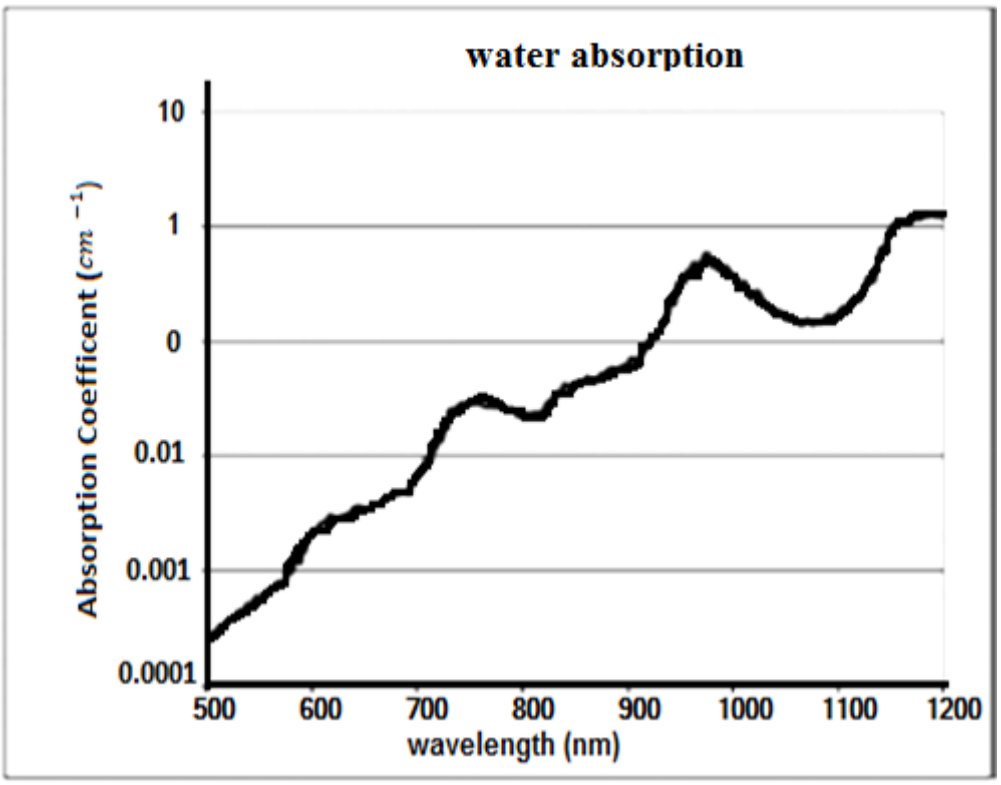

Figure (3-9): Water absorption coefficient in the range 500-1200 nm. [15]

Absorption Characteristics of Melanin

Melanin is the chromophore of the human skin epidermal layer responsible for protection from harmful UV radiation. When melanocytes are stimulated by solar radiation, melanin is produced. Melanin is one of the major light absorbers in some biological tissue (although its contribution is smaller than other components). There are two types of melanin: eumelanin which is black-brown and pheomelanin which is red-yellow. The molar extinction coefficient spectra corresponding to both types are shown in figure (3-10). [15]

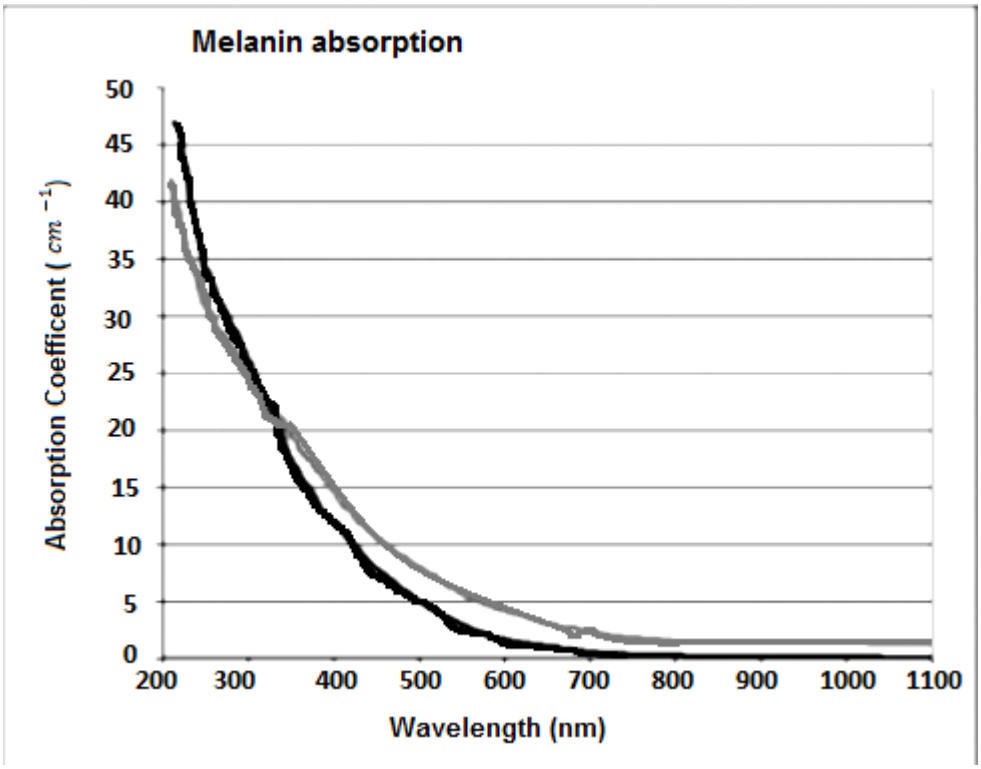

Figure (3-10): Absorption coefficient for Eumelanin (Grey curve) and Pheomelanin (black curve). [15]

The pheomelanin's absorption is higher in the short wavelength region and drops off very quickly at wavelengths higher than 700 nm. [16]

Absorption Characteristics of Skin

The skin presents a complex heterogeneous medium, where the blood and pigment content is spatially distributed with depth variations. The skin consists of three main visible layers from the surface: stratum corneum (~20μm thick), epidermis (100μm thick, the blood free layer), and dermis (1–4mm thick, vascularized layer). Figure (3-11) shows the penetration depth. Because of its thickness, dermis is the skin layer contributing the most to skin optical properties. [15]

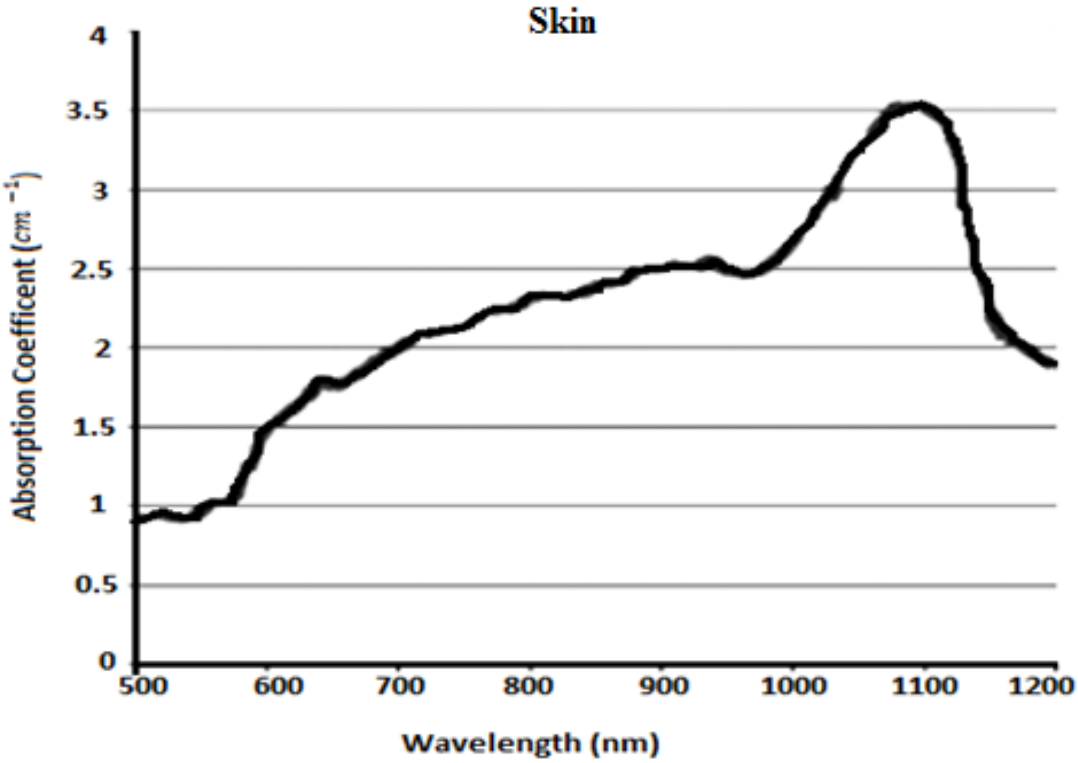

Figure (3-11): Skin optical penetration depth in the range 500-1200nm. [15]

Absorption Characteristics of Subcutaneous Adipose Tissue

The subcutaneous adipose tissue (1-6mm thick depending from the body site) is formed by aggregation of fat cells (adipocytes) containing stored fat (lipids) in the form of a number of small droplets for normal (not obese) humans. In the spaces between the cells, there are blood capillaries (arterial and venous plexus), nerves, and reticular fibrils connecting each cell and providing metabolic activity of fat tissue. Absorption of the human adipose tissue is defined by absorption of hemoglobin, lipids, and water (about 11%) (Figure (3-12)). [15]

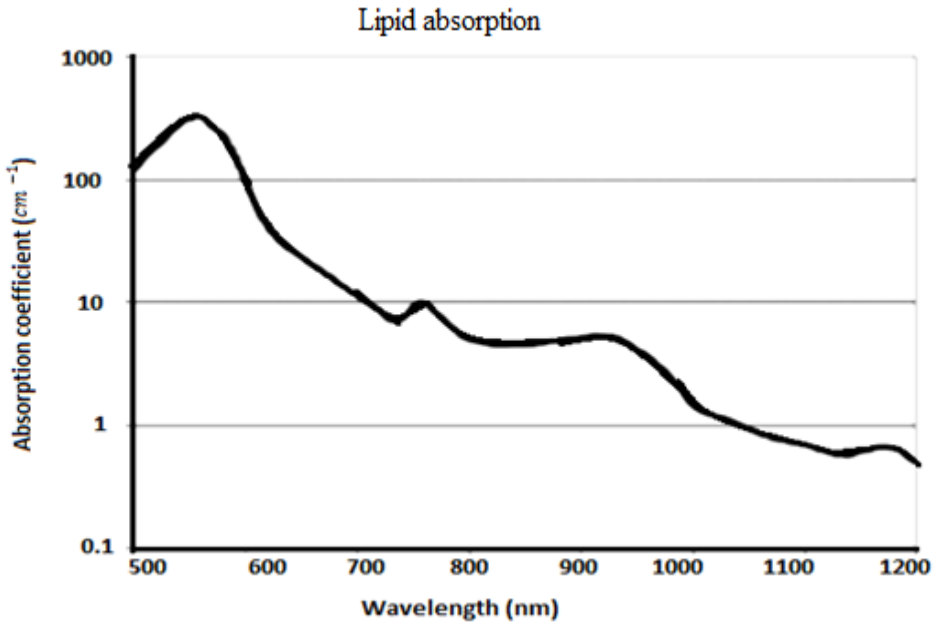

Figure (3-12): Lipid absorption coefficient in the range 500-1200nm.[15]

Absorption Characteristics of Muscles

Muscle is one of the most abundant tissues in the human body. It is well understood that muscle is made up of individual components known as muscle fibers. These fibers are made from myofibrils, which are long cylinders of few μm diameter. Absorption of the muscle tissue is defined by the absorption of hemoglobin and of water, ranging from 52 % to 73 % according to the specific muscle type and conditions (52% or 73%).[15]

Absorption Characteristics of Mucous Membrane

The proper layer of the mucous membrane is similar in structure to connective tissue, consisting of collagen and elastin fibrils. The interstitial fluid of the mucous membrane contains proteins and polysaccharides and is similar in composition to the interstitial fluid of most of the connective tissues. Figure (3-13) shows the optical penetration depth in human mucous membrane. [15]

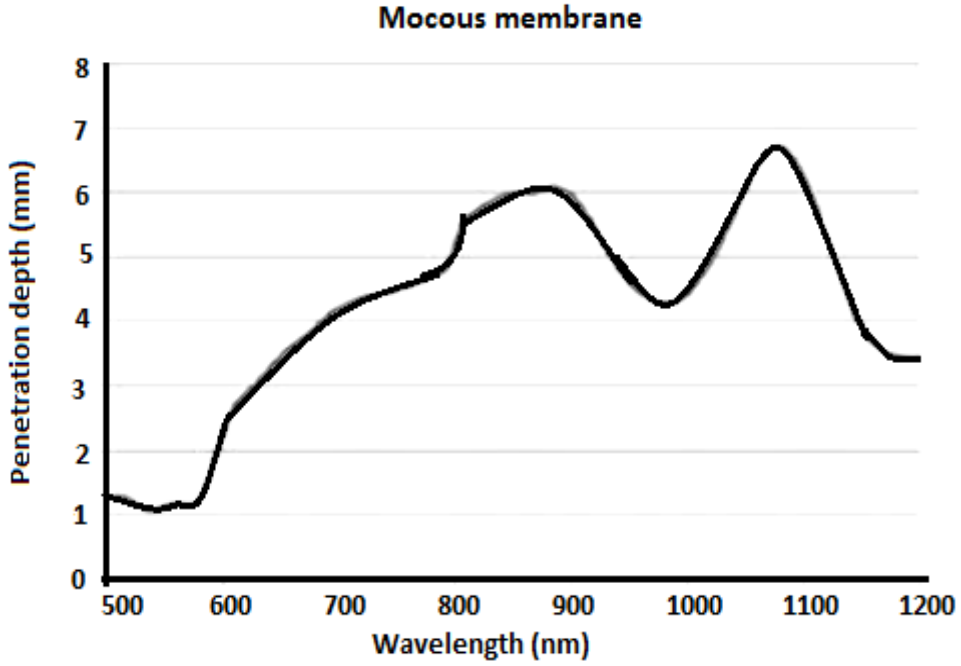

Figure (3-13): Penetration depth of 500-1200nm light in human mucous. [15]

3.5.2 Light Scattering

Scattering takes place at frequencies not corresponding to those natural frequencies of particles. The resulting oscillation is determined by forced vibration. In general, this vibration will have the same frequency and direction as that of the electric force in the incident wave. Its amplitude, however, is much smaller than in the case of resonance. Also, the phase of the forced vibration differs from the incident wave, causing photons to slow down when penetrating into a denser medium. Hence, scattering can be regarded as the basic origin of dispersion. Elastic and inelastic scattering are distinguished, depending on whether part of the incident photon energy is converted during the process of scattering. At a particular time, the electric field of the incident wave can be expressed by

$$E(z) = E_0 e^{ikz} \qquad (3\text{-}8)$$

Where E_0 is the amplitude of the incident electric field, k is the amount of the propagation vector, and z denotes the optical axis. In a first

approximation, we assume that the wave reaching some point P on the optical axis will essentially be the original wave, plus a small contribution due to scattering. The loss in intensity due to scattering is described by a similar relation as absorption, i.e.

$$I(z) = I_0 \, e^{-\mu_s z} \qquad (3\text{-}9)$$

Where μ_s is the scattering coefficient. [12]

3.5.3 Reflection and Refraction

Reflection is defined as the returning of electromagnetic radiation by surfaces upon which it is incident. In general, a reflecting surface is the physical boundary between two materials of different indices of refraction such as air and tissue. The simple law of reflection requires the wave normal of the incident and reflected beams and the normal of the reflecting surface to lie within one plane, called the plane of incidence. It also states that the reflection angle θ' equals the angle of incidence θ as shown in figure (3-14) and expressed by

$$\theta = \theta' \qquad (3\text{-}10)$$

The angles θ and θ' are measured between the surface normal and the incident and reflected beams, respectively. [12]

Refraction usually occurs when the reflecting surface separates two media of different indices of refraction. It originates from a change in speed of the light wave. The simple mathematical relation governing refraction is known as Snell's law. It is given by

$$\frac{\sin\theta}{\sin\theta''} = \frac{v}{v'} \qquad (3\text{-}11)$$

Where $\theta''$is the angle of refraction, and v and v' are the speeds of light in the media before and after the reflecting surface, respectively. [12]

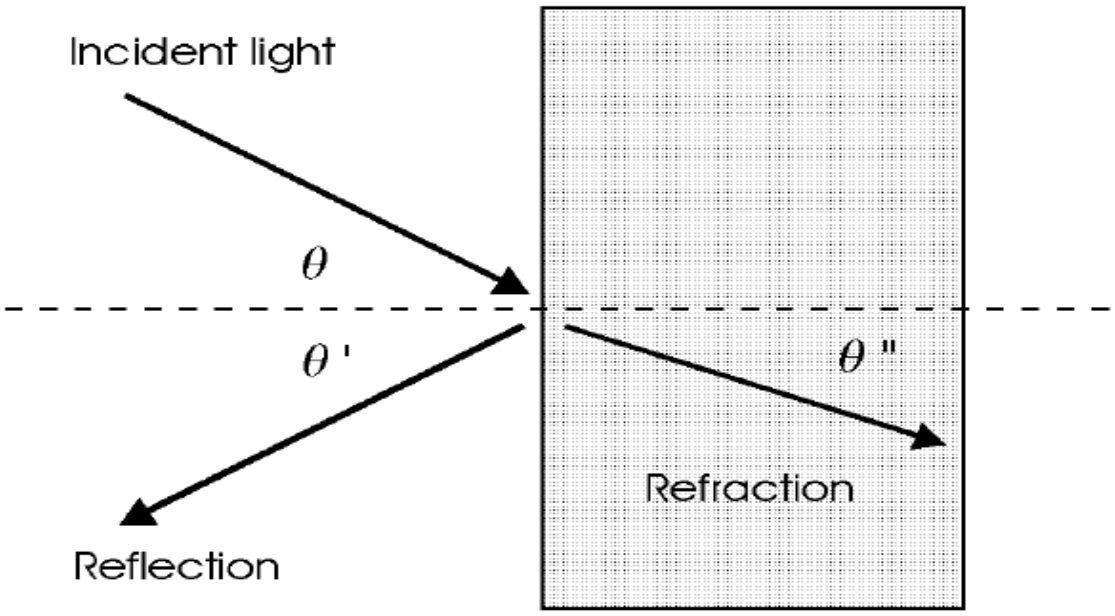

Figure (3-14): Geometry of specular reflection and refraction. [12]

Table (3-1): Optical properties of human tissues in vitro

tissue	Wavelength λ (nm)	Absorption Coefficient μ_a (cm^{-1})	scattering Coefficient μ_s (cm^{-1})
blood	665	1.3	1246
blood	685	2.65	1413
blood	960	2.84	505
Bone(skull)	488	1.4	200
Bone(skull)	514	1.3	190
Bone(skull)	1064	0.5	120
muscles	515	11.2	530
Skin(white)	633	2.7	187
Skin(white)	700	2.7	237
Skin(dark)	700	8.1	229

Chapter Four

The Proposed System

4.1 Design Concept

This chapter discusses the design of a simple prototype that used to detect Malaria type on basis of magneto-optical technology (MOT) using a permanent magnet and an infrared LASER source -which are applied to the hemozoin molecules-and embedded systems, by detecting the intensity of IR LASER absorbed beam using a data acquisition system.

4.2 Circuit Components

The proposed system basically consists of:

1. Laser diode line module.
2. Permanent magnet.
3. IR Si photodiode.
4. Operational amplifier.
5. Microcontroller.
6. LCD.
7. Breadboard power supply module.
8. Wires
9. Battery
10. Board.

Laser Diode Line Module

To generate light signal that penetrate human body, IR wavelength with 200mW/808nm length was selected based on the fact that human tissue

have low absorption factor at this range , so final selection was focusable 808nm 810nm IR Infrared 200mW Laser Diode Line Module.

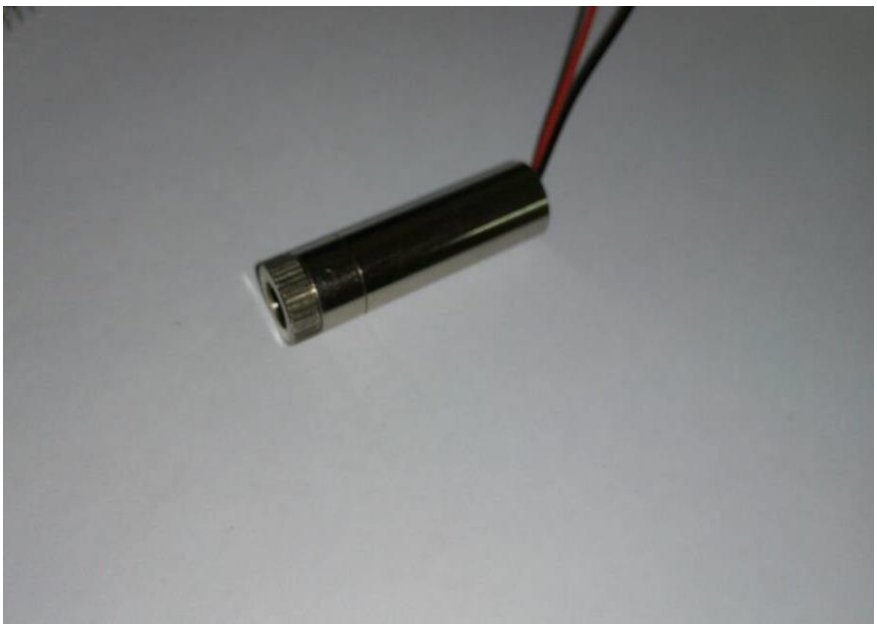

Figure (4-1) Laser diode line module

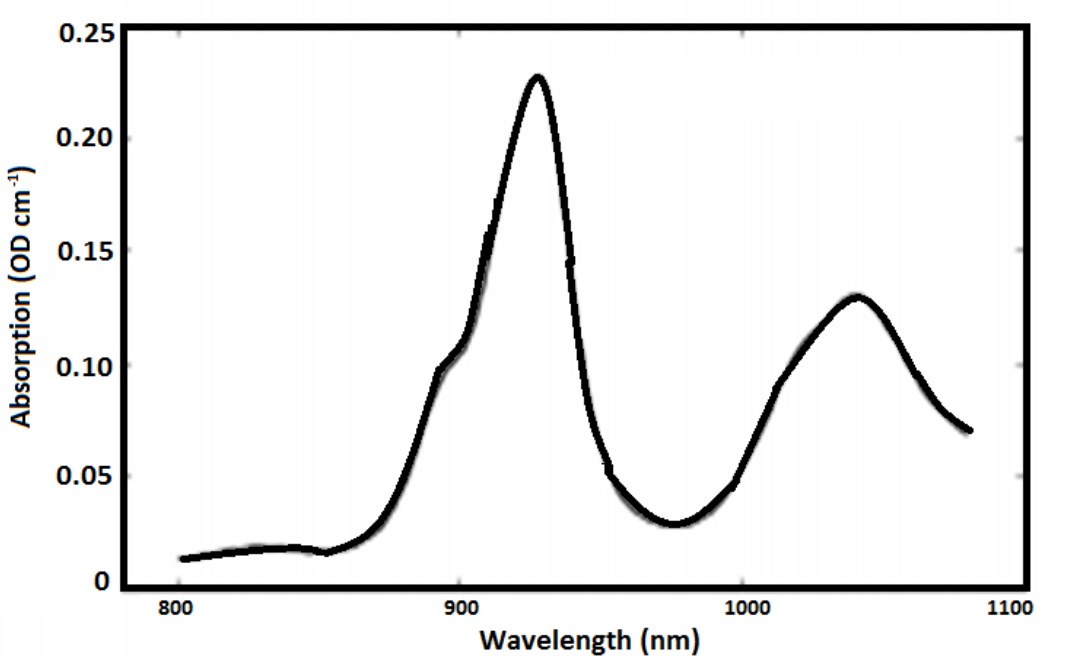

Figure (4-2): The absorption spectrum of hemozoin molecules in the IR from 800-1080nm

Permanent Magnet

In order to align hemozoin crystals 8 pieces of neodymium magnet Nd2Fe14B has been used to produce a 0.6T magnetic field.

Figure (4-3): Neodymium magnet Nd2Fe14B

Figure (4-4): 0.6T magnetic field produced by neodymium magnet Nd2Fe14B measured using teslameter

IR Si Photodiode

Si photodiode is a photodetector that has the ability to convert IR into electrical current.

This type is suited to low light level applications throughout the range 430 to 900 nm. According to the photodiode datasheet the peak DC current is 10mA with a reverse voltage up to 15v.

Figure (4-5): IR Si photodiode

Operation Amplifier

The current produced by the photodiode flows through the resistor in the op amp's feedback loop. We will see a voltage at the output of the op amp with accordance to Ohm's Law, V = I*R. The current produced by a photodiode can be pretty small (micro-amps), so this is why we are using such a large resistor (1 Mohm) as the gain-setting resistor. A high gain-resistor such as this is typical for trans-impedance amplifiers. The capacitor in the feedback loop helps reduce high-frequency noise.

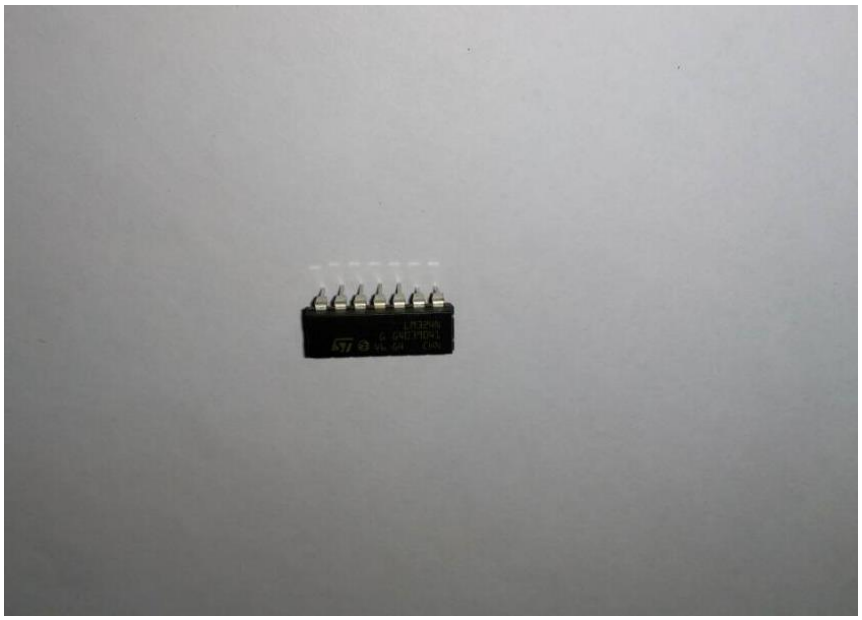

Figure (4-6): LM324 Operation amplifier

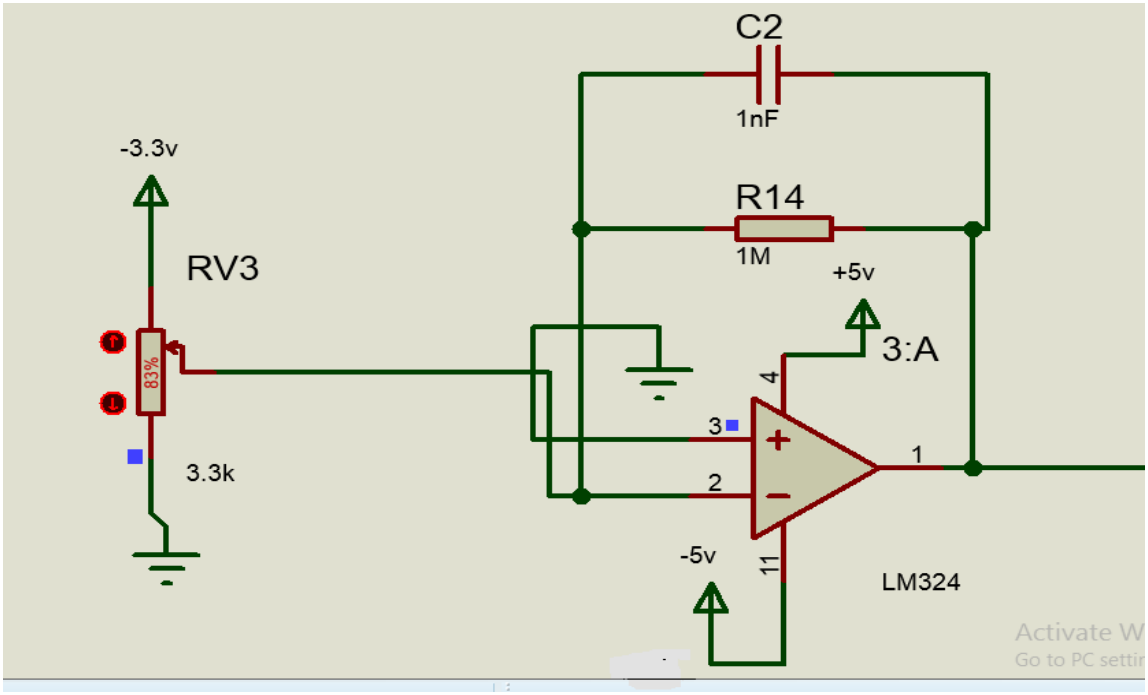

Figure (4-7): Current-voltage converter circuit

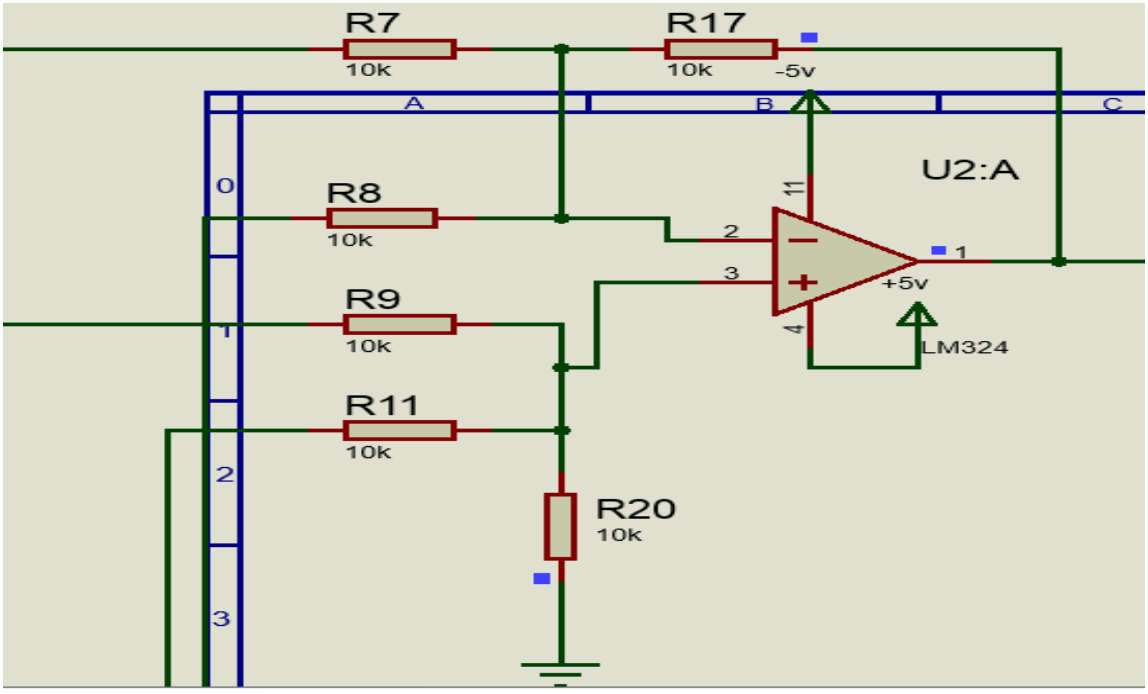

Figure (4-8): Summing and Differential amplifiers

The op-amps used were the LM324 quad type at +/-5VDC operating voltage. The output of the amplifiers are shown above and connect to the outputs of the trans-impedance amplifiers.

Microcontroller

At this research a microcontroller PIC16F877A chip -with 8KBytes In-System Programmable Flash- will be used to process the system and determine type malaria non-invasively. PIC16F877A chip is available in different types of packages. According to the type of applications and usage, these packages are differentiated.

The microcontroller pins that have been used in the circuit connection are

VCC, GND, PIND.0 and PIND.1

The microcontroller ports that have been used in the circuit connection are PORTA (as ADC), PORTB (as an output port which connected to the LCD) and PORTC (as an output port which connected to the LED).

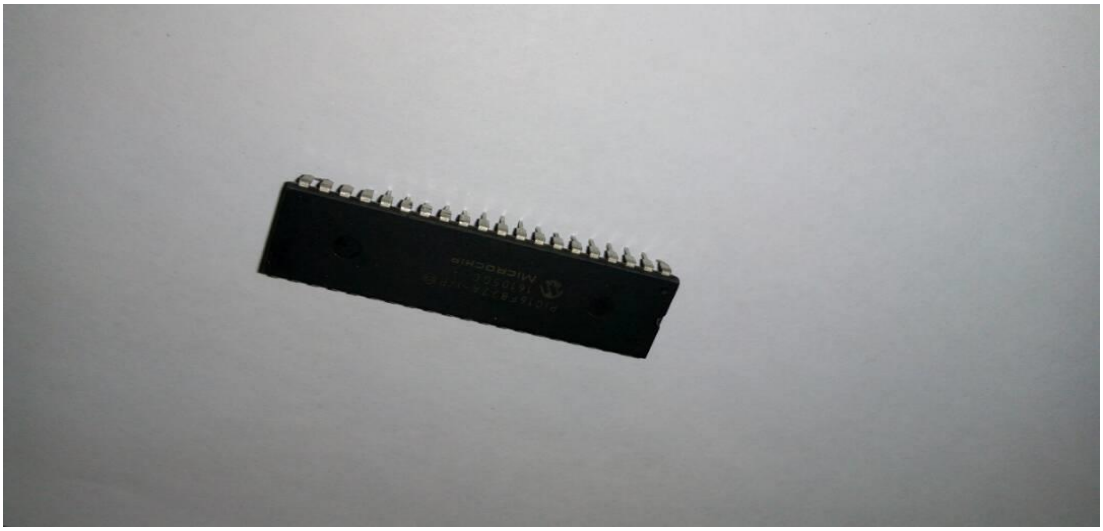

Figure (4-9): Microcontroller chip (PIC16F877A)

LCD

To display the results processed by microcontroller we used (16x2) liquid crystal display which known as LCD. (16x2) LCD means that it shows 16 character in 2 rows. The table below shows the interface between LCD and microcontroller.

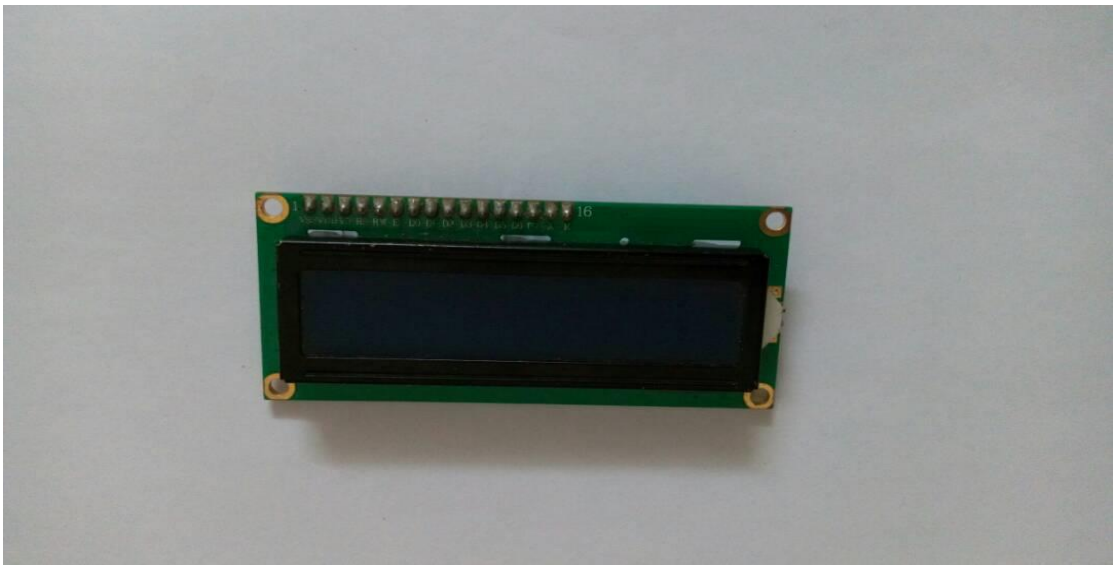

Figure (4-10): LCD

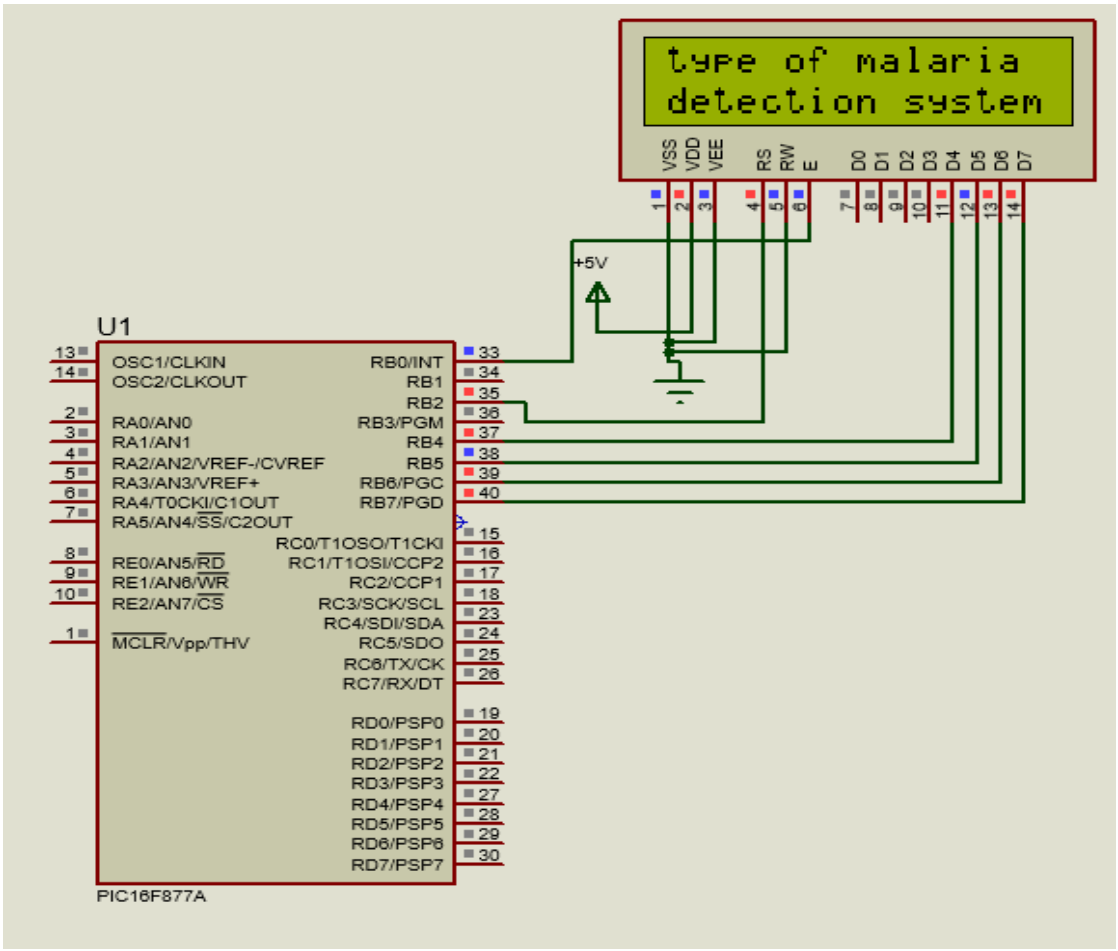

Figure (4-11): Interfacing LCD with PIC16F877A microcontroller chip

Table (4-1): LCD pin interfacing with microcontroller.

Pins of port D	LCD pins
Pin 0	EN
Pin 2	RS
Pin 4	B4
Pin 5	B5
Pin 6	B6
Pin 7	B7

Breadboard Power Supply Module

In order to generate 3.3V needed by Laser diode line module we used breadboard power supply module. The module can take 6.5V to 12V DC input to produce 3.3V and +5V with a maximum output current <700 mA. The module has 2 × 1×4 selection jumper for 3.3 / OFF / 5V.

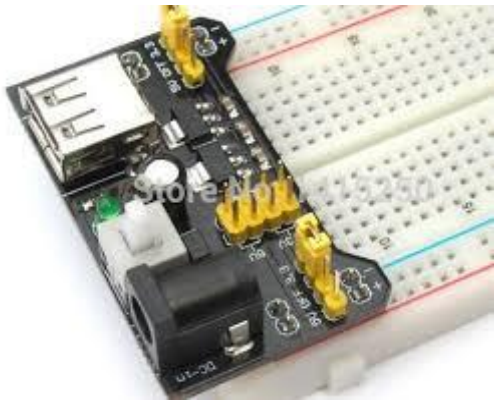

Figure (4-12): Breadboard power supply module

4.3 Cuvette Design

The second part of our prototype is black cuvette which has been made from Teflon. The main function of this part is to prevent outside

environment light to interact with laser beam. Figure below shows the dimensions of the cuvette which designed using solid work software.

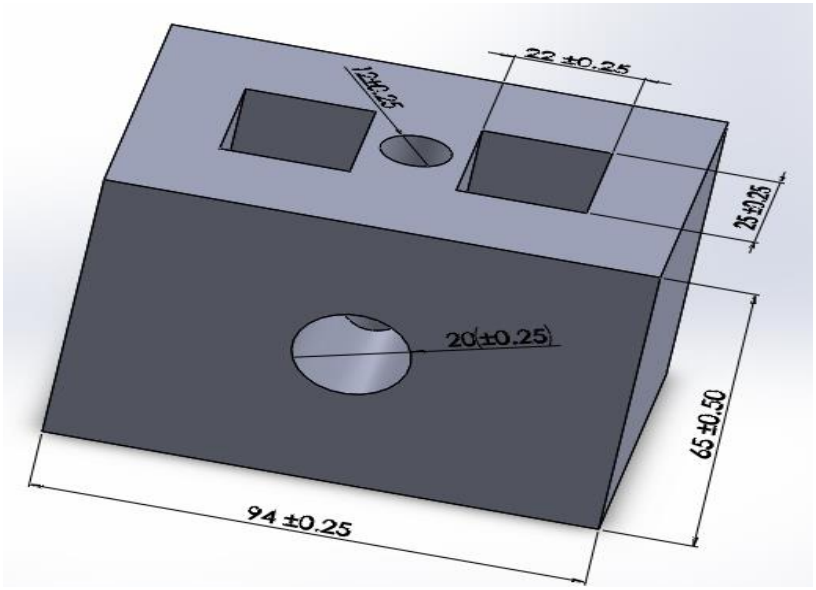

Figure (4-13): Black Teflon cuvette 3D image

Teflon Characteristics

The specific characteristics of Teflon are:

1. A white waxy substance.
2. Strong resistance to chemical acid.
3. Smooth surface.
4. It retains physical properties unchanged at temperatures ranging from 270- to 250 Silesia.
5. Insulating material for electricity.
6. To dissolve in organic solvents.
7. A flexible material.

4.4 Block Diagram

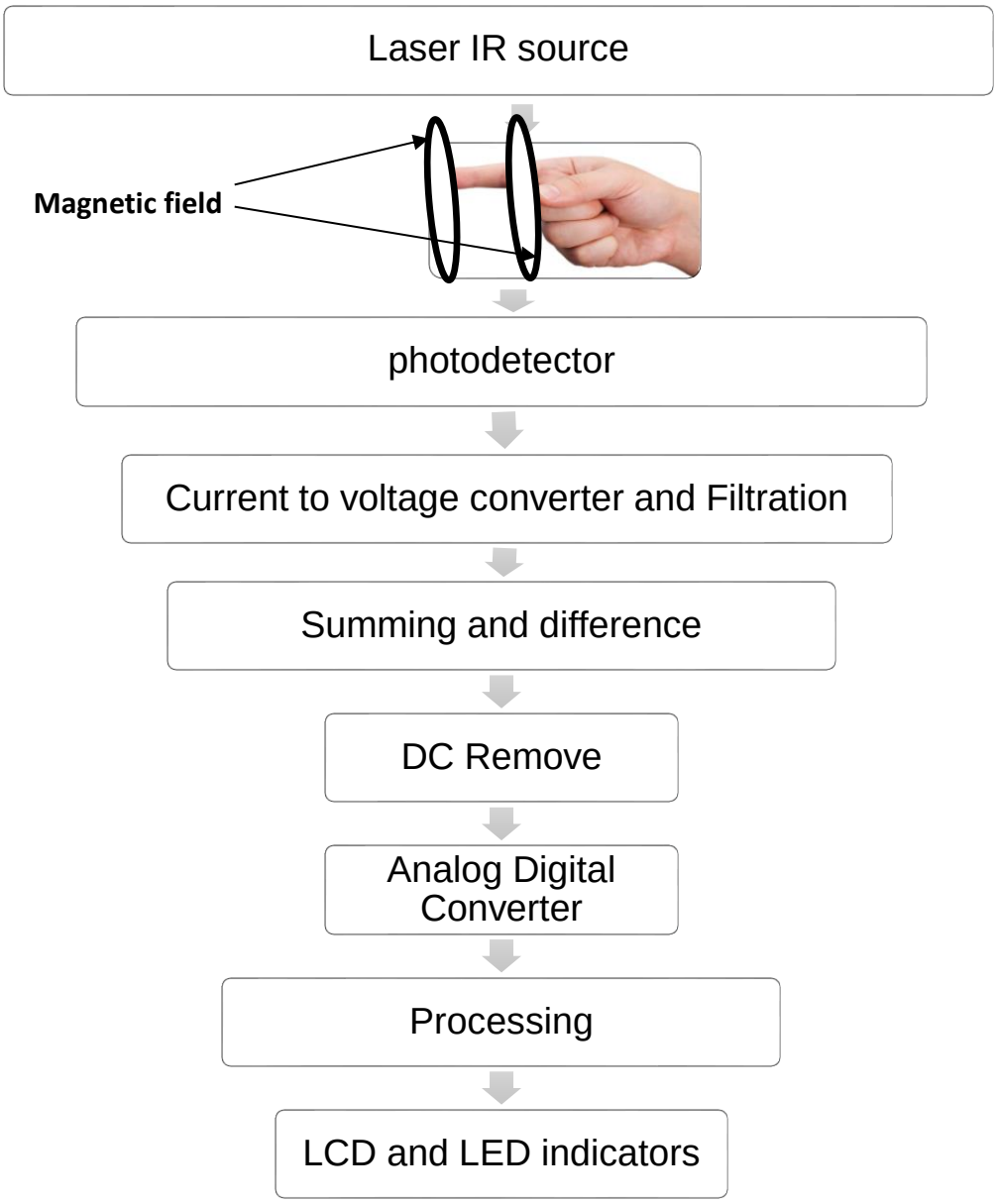

Figure (4-14): Block diagram of the proposed system

4.5 MikroC PRO programme

The mikroC PRO for PIC is a powerful, feature-rich development tool for PIC microcontrollers. It is designed to provide the programmer with the easiest possible solution to developing applications for embedded systems, without compromising performance or control.

4.6 Algorithm

The algorithm of Invasive Detection – blood sample- Algorithm shows the steps of the software program of the proposed system

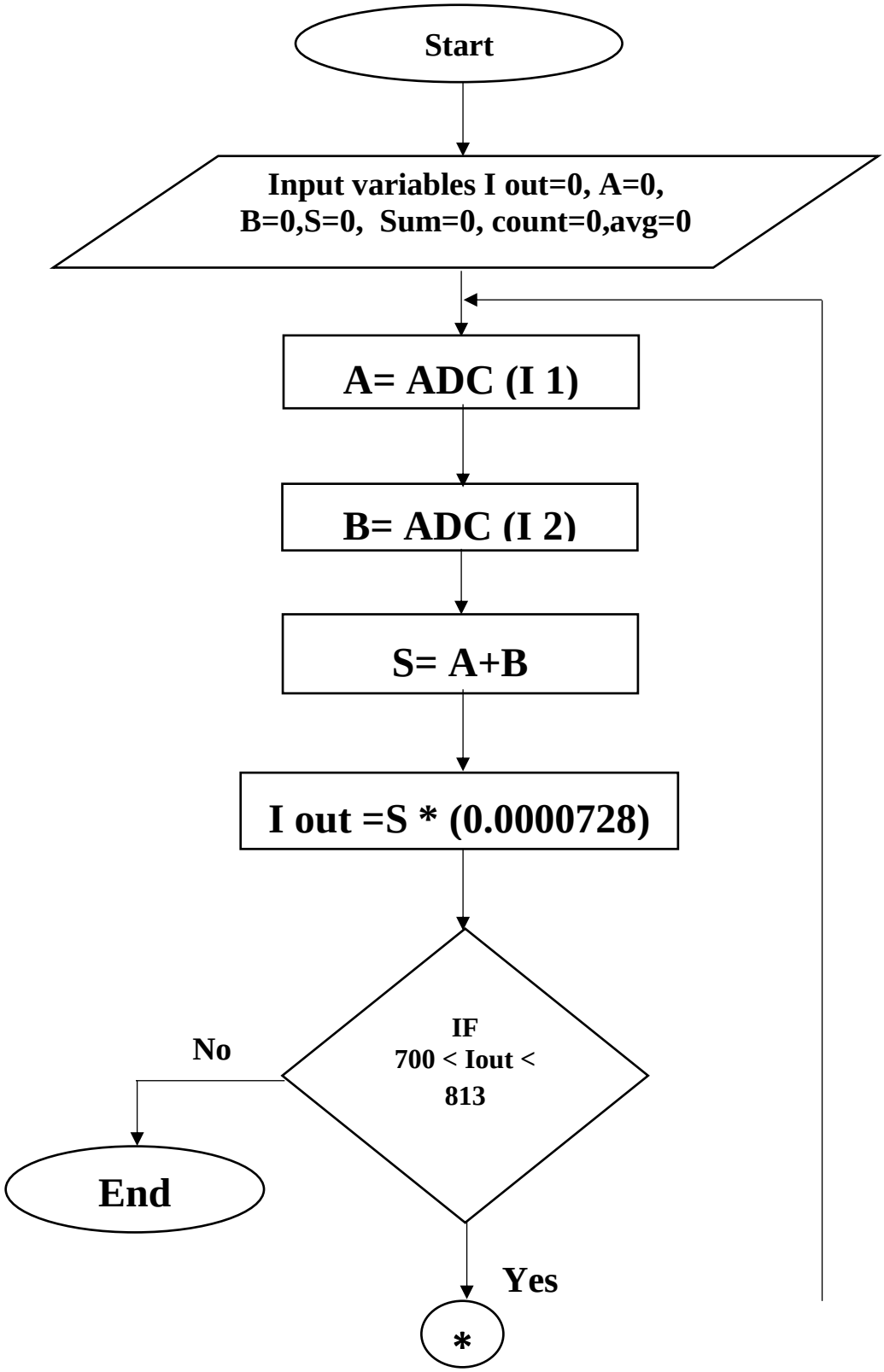

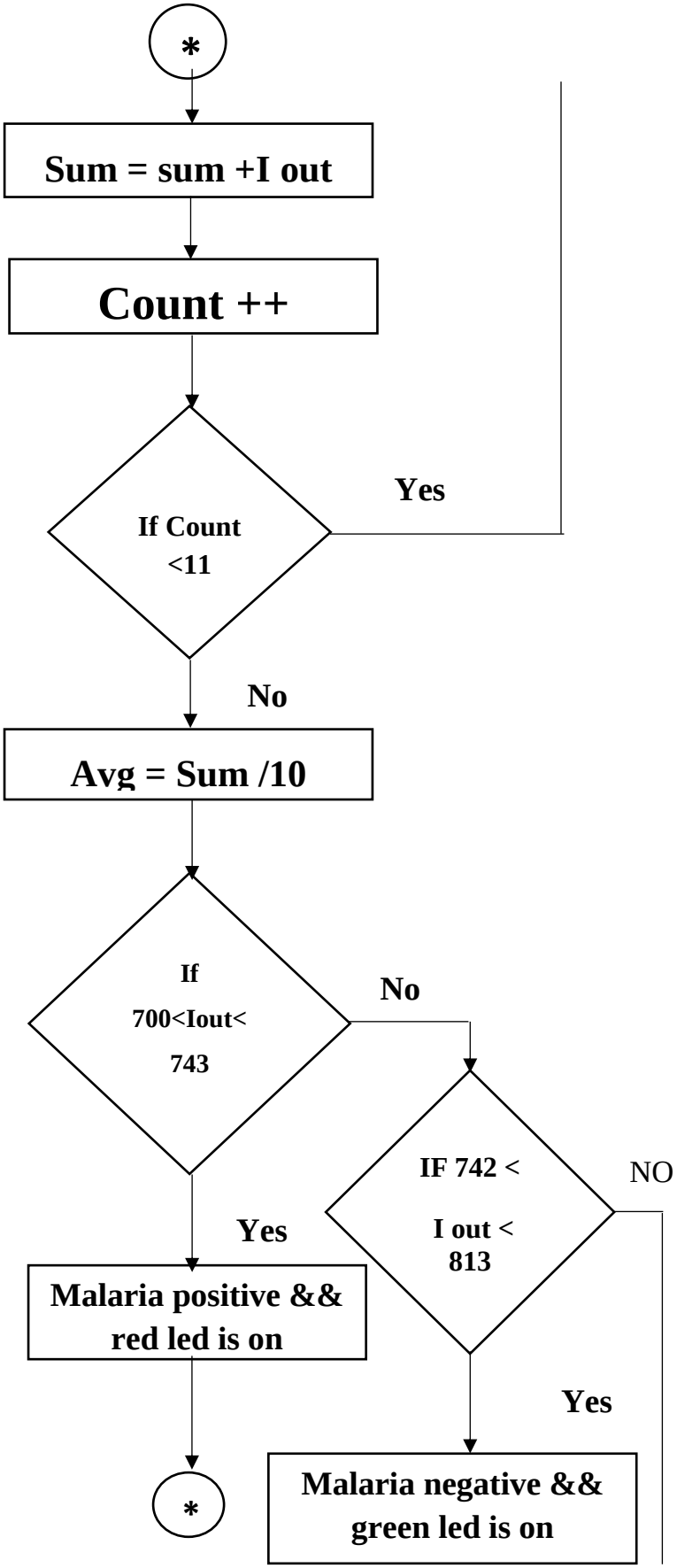
*
Sum = sum +I out
Count ++
If Count <11
Yes
No
Avg = Sum /10
If 700<Iout< 743
No
IF 742 < I out < 813
NO
Yes
Malaria positive && red led is on
Yes
Malaria negative && green led is on
*

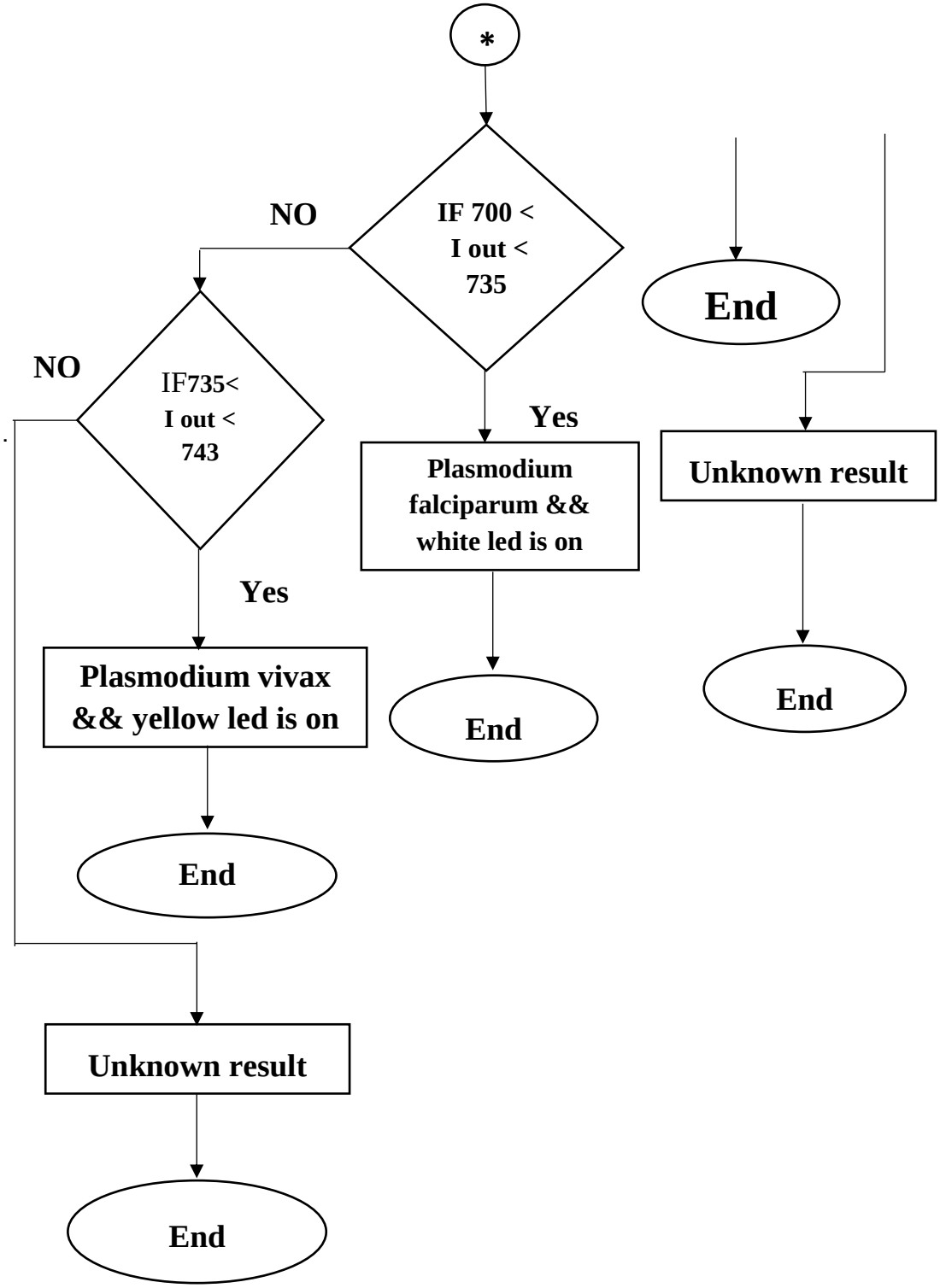
*
IF 700 < I out < 735
NO
IF735< I out < 743
NO
Yes
Plasmodium vivax && yellow led is on
End
Unknown result
End
Yes
Plasmodium falciparum && white led is on
End
End
Unknown result
End

The algorithm of non-Invasive Detection –index finger- Algorithm shows the steps of the software program of the proposed system

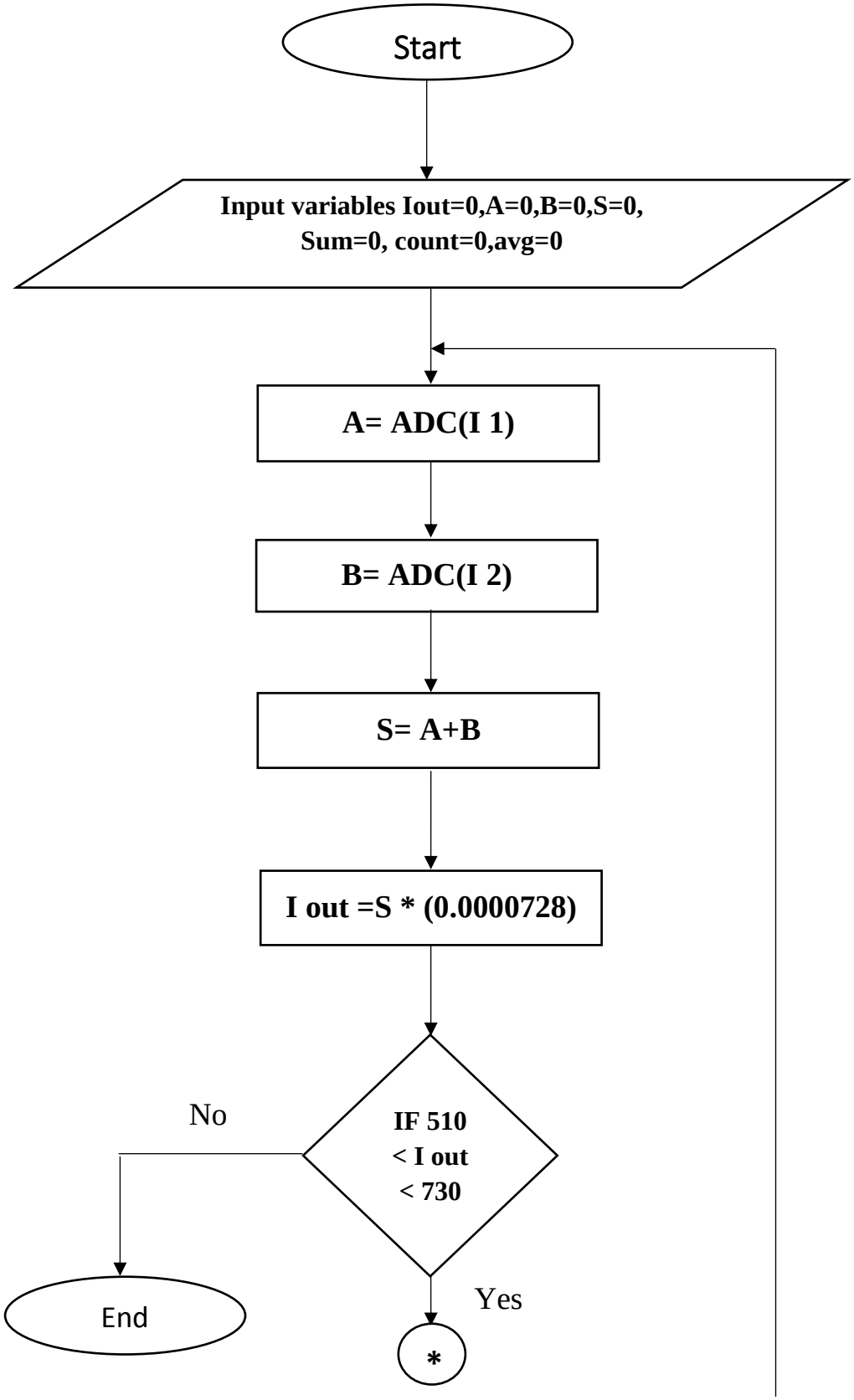

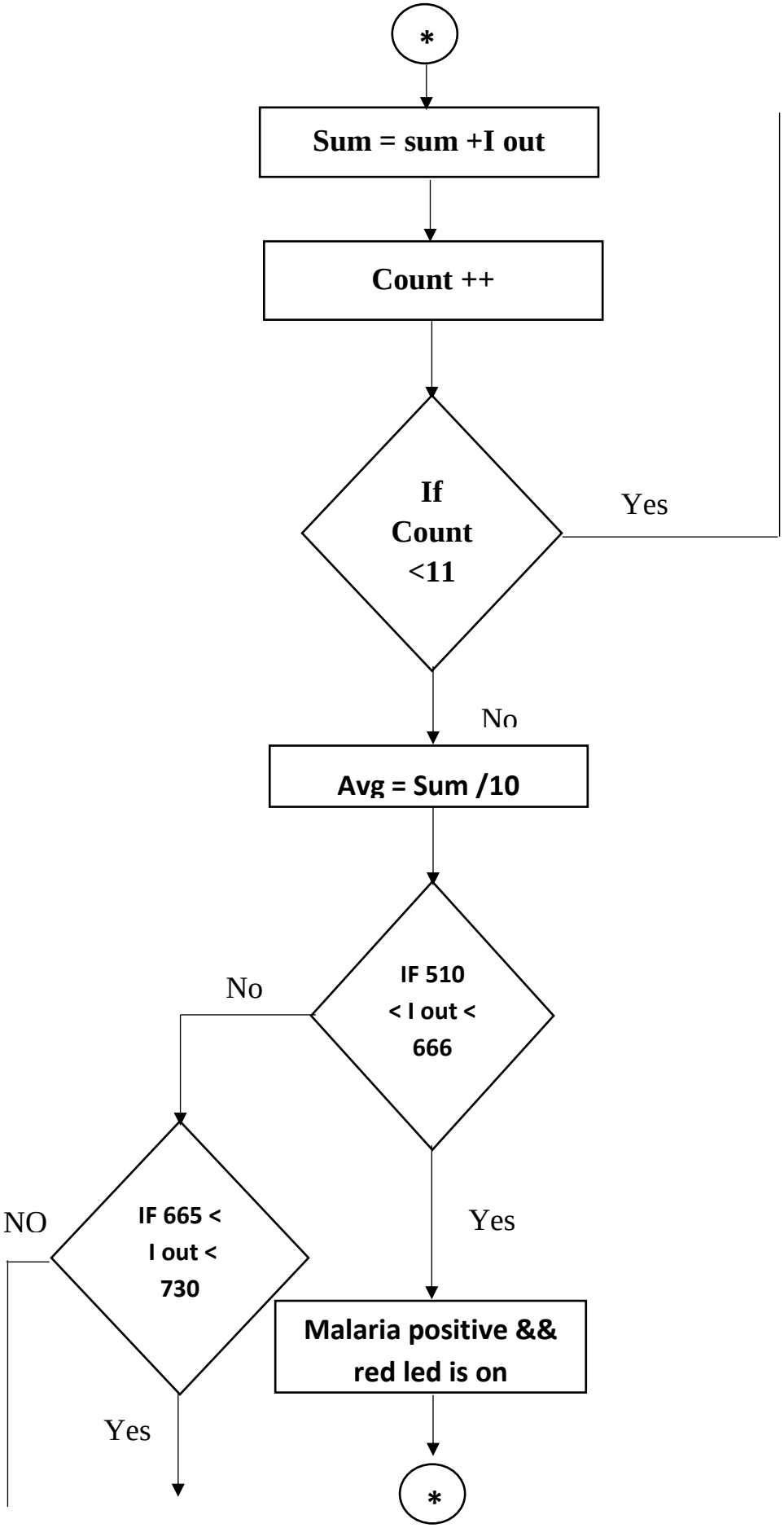
*
Sum = sum +I out
Count ++
If Count <11
Yes
No
Avg = Sum /10
IF 510 < I out < 666
No
IF 665 < I out < 730
NO
Yes
Yes
Malaria positive && red led is on
*

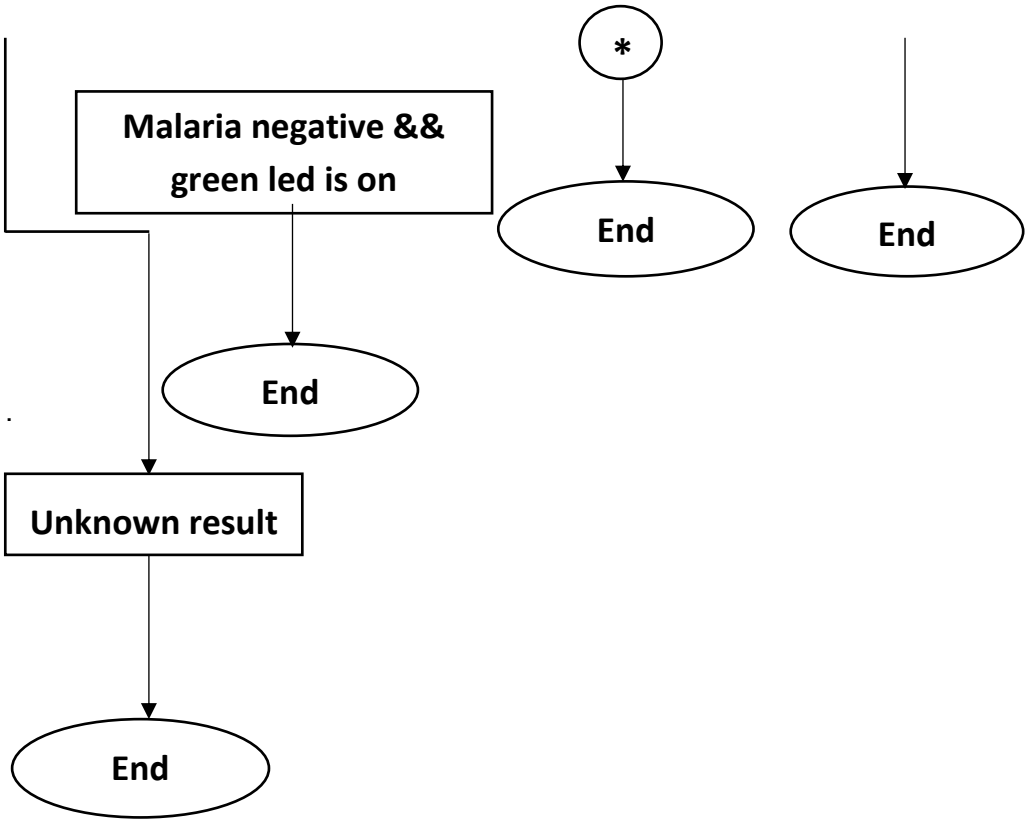

4.7 Simulation

In order to validate the functionality of the prototype, a simulation circuit has been designed using PROTEUS 8.0 software.

Every electronic component that have been used in the real circuit, were selected in the simulation circuit to give the same function of the proposed system.

As shown in the figure (4-15) the laser source was replaced with DC 3.3V voltage source which represents the voltage needed to supply laser module in the real circuit. Also the Si photodiode was replaced with potentiometer as in the real circuit when the light intensity is received by the photodiode, the current that passes to the operational amplifier will also change which is the same function of potentiometer.

The system is designed to operate in two modes, invasive and non-invasive, which is determined via a pair of switches. Also a set of four LEDs were added to indicate the presence and the type of malaria.

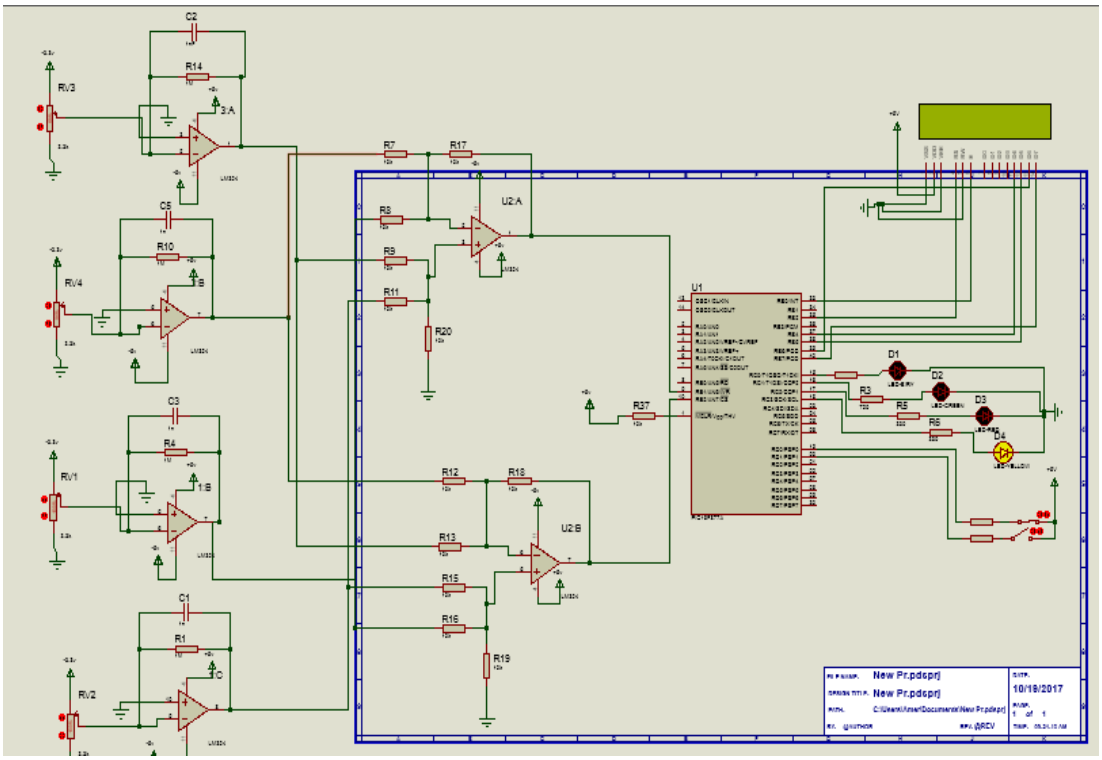

Figure (4-15): Whole circuit simulation

4.8 Mathematical Model

1. Wavelength source is 810 nm.
2. Complete width of the index finger is 20 mm.
3. Distance between source and index finger is 3mm, in addition index finger to detectors is 30mm.
4. Calculations done depend on Mie and Millar const.

Table (4-2): absorption coefficient of finger

layer	thickness	absorption coefficient (μ_a)
skin	3.1 mm	5.4 cm^{-1}
muscle	1.5 mm	11.2 cm^{-1}
blood	8 µm	2.84 cm^{-1}
bone	10 mm	0.5 cm^{-1}

1. **Skin:**

$$I_o = I_{in}\, e^{-\sum \mu_a * d}$$

μ_a= 5.4 cm^{-1} , d =3.1 mm:

$$5.4 * 10^2 * 3.1 * 10^{-3} = \ 1.68021$$

2. **Muscle:**

μ_a= 11.2 cm^{-1} , d =1.5 mm :

$$11.2 * 10^2 * 1.5 * 10^{-3} = \ 1.68$$

3. **Blood :**

μ_a= 2.84 cm^{-1} , d =8 µm :

$$2.84 * 10^2 * 8 * 10^{-6} = \ 2.272 * 10^{-3}$$

4. **Bone :**

μ_a= 0.5 cm^{-1} , d =10 mm :

$$0.5 * 10^2 * 10 * 10^{-3} = \ 0.5$$

$$\therefore I_o = I_{in} * \ e^{-(2(1.68021)+2(1.68)+2(2.272*10^{-3})+(0.5))}$$

$$\therefore I_o = I_{in}\, e^{-7.224964}$$

For skin, muscle and blood so we multiply it with 2.

4.9 Implementation

The circuit applied as in figure (4-16) shows the implemented prototype:

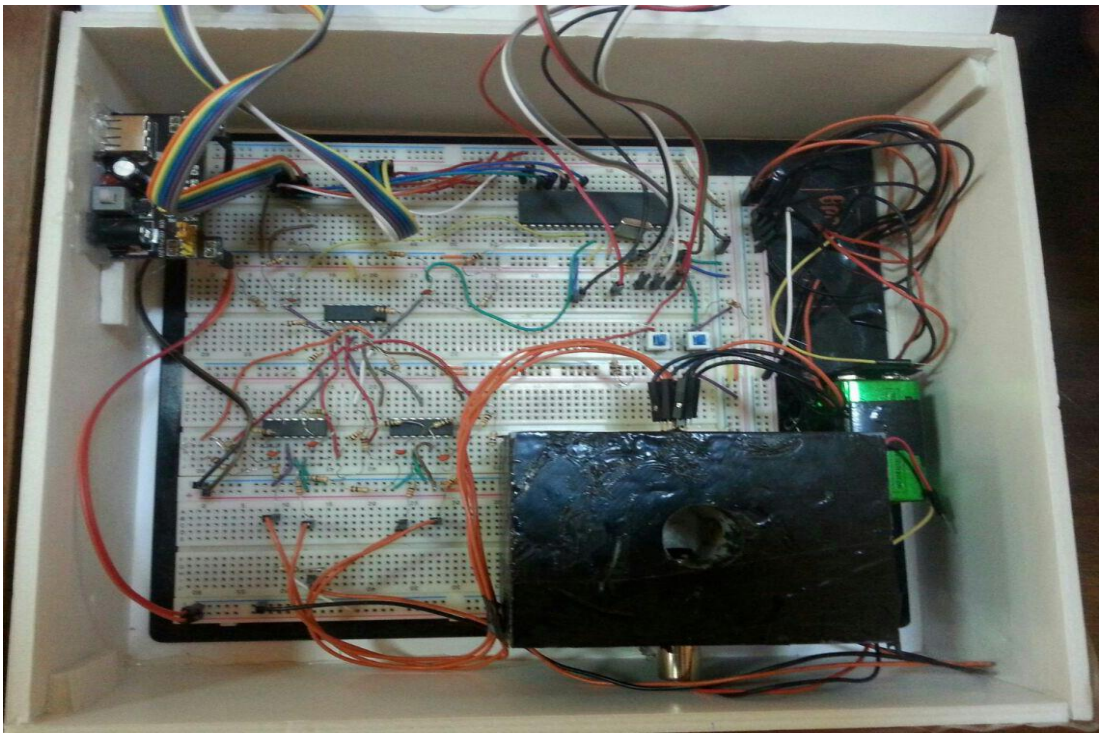

Figure (4-16): The implemented prototype

A blood sample tube or finger had been placed in the hole between the photodetector and the LASER light aperture inside the cuvette, when the LASER light strikes the sample or finger; the hemozoin particles –which are already aligned in the direction of magnetic flux- the absorption light will be detected by the photodetector which converts these changes in intensity to small current then its converted to a voltage via current to voltage converter circuit. These voltage values will be sent to the microcontroller as input via ADC pins, then the microcontroller program calculates the intensity of light according to based-in algorithms (this determine whether malaria is positive or negative), the result will be displayed on the LCD in term of millivolts. A 12v adapter or a 5v battery charger used to supply the microcontroller and 9v reverse battery used to supply the photodiode. Also two switches and four LEDs are used.

Chapter Five

Experiments Results

5.1 Result 1

The circuit was tested firstly on twenty one blood sample. Table (5-1) shows the results of samples test.

Table (5-1): Results of invasive test

Sample No.	Laboratory results	Experiment results	Type
1	Negative	Negative	-
2	Negative	Negative	-
3	Negative	Negative	-
4	Negative	Negative	-
5	Negative	Negative	-
6	Negative	Negative	-
7	Negative	Negative	-
8	Negative	Negative	-
9	Negative	Negative	-
10	Negative	Positive	-
11	Positive	Positive	P.vivax
12	Positive	Positive	P. falciparum
13	Positive	Positive	P. falciparum
14	Positive	Positive	P. falciparum
15	Positive	Positive	P. falciparum
16	Positive	Positive	P. falciparum
17	Positive	Positive	P. falciparum
18	Positive	Positive	P. falciparum
19	Positive	Positive	P. falciparum
20	Positive	Positive	P. falciparum
21	Positive	Positive	P. falciparum

5.2 Discussion 1

A total of twenty one blood samples were taken from several hospitals and laboratories, and they were re-tested by the prototype as seen in table (5.1), nine of them were in the negative range (743 to 812 mV) and one sample was negative but had a value in the positive range (729 mV). Ten of the total samples had the same plasmodium species (P. falciparum) which were in the range of (701 to 734mV) and one sample was (p.vivax) which had a value in the range of (735 to 742 mV) inside the positive range (701 to 742 mV).

$$\text{Accuracy} = \frac{Number\ of\ correct\ samples}{Number\ of\ all\ samples} * 100\%$$

$$\text{Accuracy} = \frac{20}{21} * 100\% = 95.24\%$$

5.3 Result 2

The circuit then was tested on seventeen cases. Table (5-2) shows the results of the tests.

Table (5-2): Results of non-invasive test

Patient No.	Laboratory results	Experiment results	Type
1	Negative	Negative	-
2	Negative	Negative	-
3	Negative	Negative	-
4	Negative	Negative	-
5	Negative	Negative	-
6	Negative	Negative	-
7	Negative	Negative	-
8	Negative	Negative	-
9	Negative	Negative	-
10	Negative	Unknown	-
11	Positive	positive	P. falciparum

12	Positive	Negative	P. falciparum
13	Positive	Positive	P. falciparum
14	Positive	Positive	P. falciparum
15	Positive	Positive	P. falciparum
16	Positive	Positive	P. falciparum
17	Positive	Positive	P. falciparum

5.4 Discussion 2

A total of seventeen cases were tested by the prototype as seen in table (5.2), nine of them were in the negative range (666 to 729 mV) and one sample was negative but had a value out of detection range (496 mV). Seven of the total samples had the same plasmodium species (P. falciparum) which were in the range of (511 to 665mV).

$$\text{Accuracy} = \frac{Number\ of\ correct\ results}{Number\ of\ all\ results} * 100\%$$

$$\text{Accuracy} = \frac{15}{16} * 100\% = 93.75\%$$

The unknown result has been neglected.

Chapter Six

Conclusion and Recommendations

6.1 Conclusion

In this project invasive and non-invasive techniques were merged in one system to detect all common types of malaria depending on basis of magneto-optical technique (MOT) [using a magnetic field and laser "Infrared waves"] and embedded systems, by detecting IR LASER beam passing through human finger or blood sample.

The proposed system used to test (21) blood samples with (9) negative samples and (12) positive samples and lead to results with accuracy (95.24%), then it used to test (17) persons, (9) of them were non-infected, (7) were infected and one was unknown case which conclude to results with accuracy (93.75%) .

6.2 Recommendations

From this study there are four recommendations for further studies:

1- Use the proposed system to test the other two types of plasmodium.
2- Design an adjustable testing hole for finger so that the device is able to perform for various sizes of fingers.
3- Adding a memory to the device to provide the ability of saving test results.
4- Manufacture the device for clinical uses.

References

[1] Gunnar Holmgren, “Malaria the disease of fours”, Infectious diseases clinic, Ryhov Hospital, Jönköping, , Sweden, Feb. 2015

[2] “Understanding malaria. U.S. Department of health and human services, National Institute of Allergy and Infectious Diseases” ,NIH Publication No. 07-7139. February 2007.

[3] “UNAIDS-Basic Malaria Microscopy”, Second Edition-Part I, Learner's Guide, 2010.

[4] Payne D.,”Use and limitations of light microscopy for diagnosing malaria at the primary health care level”, Bulletin of the World Health Organization, 1988, 66:621–626.

[5] Joel C. Mouatcho and J. P. Dean Goldring , “Malaria rapid diagnostic tests: challenges and prospects” , Department of Biochemistry, School of Life Science, University of Kwazulu-Natal, Pietermaritzburg, Private Bag X01 Scottsville 3209, South Africa,2013.

[6] Robert H. Yolken,” Enzyme Immunoassays for the Detection of Infectious Antigens in Body Fluids: Current Limitations and Future Prospects”, 1982.

[7] https://www.google.ch/imgres?imgurl=http%3A%2F%2Fiscience mag.co.uk .

[8] Peipei Li, Zhenjun Zhao, Ying Wang, Hua Xing, Daniel M Parker, Zhaoqing Yang, Elizabeth Baum, Wenli Li, Jetsumon Sattabongkot, Jeeraphat Sirichaisinthop , Shuying Li, Guiyun Yan, Liwang Cui and Qi Fan , “Nested PCR detection of malaria directly using blood filter paper samples from epidemiological surveys” , 2011

[9] Ofentse Jacob Pooe,”The detection of Plasmodium falciparum in human saliva samples”,South Africa. Dissertation submitted to the

department of Biochemistry and Microbiology. Faculty of Science and Agriculture at University of Zululand, February 2011.

[10] Wilson NO, Adjei AA, Anderson W, Baidoo S, Stiles JK ,"Detection of Plasmodium falciparum histidine-rich protein II in saliva of malaria patients", Atlanta at USA. Morehouse School of Medicine. Department of Microbiology. Biochemistry and Immunology, 2004.

[11] Kwannan Nantavisai," Malaria detection using non-blood samples Department of Microbiology", Faculty of Medicine, Srinakharinwirot University, Watthana, Bangkok, Thailand, 2014.

[12] Markolf H. Niemz, "Laser-Tissue Interactions Fundamentals and Applications", Third Enlarged Edition, 2003.

[13] Dean, J.A , "Lange's Handbook of Chemistry", 14th Edition,., McGraw-Hill, Inc., New York, Ed.1992.

[14] Weast, R.C,"Handbook of Chemistry and Physics", 56th Edition, CRC Press, Cleveland, Ed. 1975.

[15] G. Romano1, A. Conti, A. Gnerucci, P. Imperiale, F. Fusi," Laser-tissue interaction principles: tissue optical properties in the light therapeutic window (invited review)", 2014.

[16] Gregory B. Altshuler, PhD. Ilya Yaroslavsky, PhD. Palomar Medical Technologies, "Absorption Characteristics of Tissues as a Basis for the Optimal Wavelength Choice in Photodermatology", 2004.

[17] En Yong Wang, Zhen Gpin Gou, Ai-Min Miao, Shu-ging peng, Zhen yong niu and Xin linshi , "Recognition of Blood Cell Images Based on Color Fuzzy Clustering", 2009. Vol 62. pp 69-75.

[18] Ahmed el-mubarak Bashir, Zeinab A.Mustafa, Islah Abdelhameid, Rimaz Ibrahem," Detection of Malaria Parasites Using Digital Image Processing", 2017.

[19] Lukianova-Hleb, E., Bezek, S., Szigeti, R., Khodarev, A., Kelley T., Hurrell, A.Lapotko,’’ D.,Transdermal Diagnosis of Malaria Using Vapor Nanobubbles”, 2015.

[20] J. Jones, R. Deissler, W. Condit, B. Grimberg, and R. Brown, "Studying the magnetic and optical properties of Malaria for use in Early Detection," Senior project thesis, Case Western Reserve University, 2012.

[21] F.Boray Tek, Andrew.G Dempster ,and Izzet Kale, “Computer vision for microscopy diagnosis of malaria”, 2009.

[22] https://www.researchgate.netprofileTeun_Bousemapublication510 41525figurefig1AS277178781585412@1443095979757FIG-1-Top-Life-cycle-of-Plasmodium-falciparum-and-gametocyte-development-Malaria.png.

[23] https://globalhealth.duke.edu/sites/default/files/styles/dghi_medium/public/field/image/cell_image_weinberg_cropped.jpg?itok=ctnjcel7.

[24] https://learnzoology.files.wordpress.com/2014/03/p-vivax-mature-macrogametocyte.jpg.

[25] https://images.search.yahoo.com/yhs/search;_ylt=AwrB8pPSiehZpwQAAMY2nIlQ?ei=UTF8&n=60&type=9653490_SD_us&fr=yhs-visicom-weathernow&hsimp=yhs-weathernow&hspart=visicom&p=P.+malariae%2C+Band+shaped+trophy&fr2=sp-qrw-corr top&norw=1#id=71&iurl=http%3A%2F%2Fwww.fiocruz.br%2Fioc%2Fmedia%2F2008_01_07_malaria_plasmodium_vivax.jpg&action=click